Three Dimensional Modeling of Flexible Pavements

Final Report
March 2002

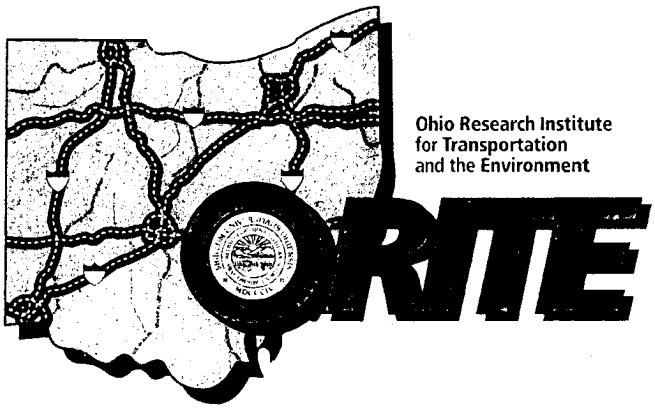

Stocker Center
Ohio University
Athens, OH
45701-2979

1. Report No.	2. Government Accession No.	3. Recipient's Catalog No.
FHWA/HWY-02/2002		

4. Title and SubtitleL	5. Report Date
Three Dimensional Modeling of Flexible Pavements	August, 2001
	6. Performing Organization Code
	8. Performing Organization Report No.

7. Author(s)	10. Work Unit No. (TRAIS)
Shad Sargand	

9. Performing Organization Name and Address	11. Contract or Grant No.
Department of Civil Engineering Ohio University 114 Stocker Center Athens, OH 45701	State Job No. 14654(0)
	13. Type of Report and Period Covered Final Report

12. Sponsoring Agency Name and Address	14. Sponsoring Agency Code
Ohio Department of Transportation 1980 W Broad Street Columbus, OH 43223	

15. Supplementary Notes

16. Abstract

A linear viscoelastic model has been incorporated into a three-dimensional finite element program for analysis of flexible pavements. Linear and quadratic versions of hexahedral elements and quadrilateral axisymmetrix elements are provided. Dynamic problems are solved by explicit, implicit, or combined explicit-implicit integration methods. Results from the program are shown to compare favorably with data from the Ohio test road.

17. Key Words	18. Distribution Statement
viscoelastic, flexible pavement, OUPAVE, 3-D finite element	No Restrictions. This document is available to the public through the National Technical Information Service, Springfield, Virginia 22161

19. Security Classif. (of this report)	20. Security Classif. (of this page)	21. No. of Pages	22. Price
Unclassified	Unclassified		

THREE DIMENSIONAL MODELING OF FLEXIBLE PAVEMENTS

FINAL REPORT

Prepared for the

OHIO DEPARTMENT OF TRANSPORTATION

And

FEDERAL HIGHWAY ADMINISTRATION

By

Shad M. Sargand
Russ Professor
Civil Engineering Department

And

David Beegle
Graduate Student
Civil Engineering Department

Ohio University
Ohio Research Institute for Transportation and the Environment
Athens, Ohio University

March 2002

Contents

List of Figures

List of Tables

CHAPTER 1

Introduction

A finite element program has been developed to study the response of flexible pavement to static and dynamic loading. Fully three-dimensional analyses can be carried out with linear or quadratic hexahedral elements having up to twenty nodes. Linear and quadratic axisymmetric elements are also furnished for rapid problem-solving. Chapter 2 describes the hexahedral elements, and Chapter 3 describes the axisymmetric elements. Both a linear elastic model and a linear viscoelastic model are provided. The material models are discussed in Chapter 4.

Chapter 5 explains the solution procedure for static and dynamic problems, including the explicit and implicit integration methods. The central difference method, used for explicit integration, is unstable unless the time step is below a critical value. The program estimates the critical value quickly by two methods instead of computing it directly. The advantage of the central difference method is that it requires relatively few operations per iteration, but the disadvantage is that it requires relatively many iterations.

The implicit integration is done with Newmark's method. This method is unconditionally stable, so accuracy—not stability—is the only criterion in choosing the time step. The advantage and disadvantage of Newmark's method are the opposite of those for the central difference method: Newmark's method requires relatively few iterations but relatively many operations per iteration.

The explicit and implicit integration schemes can be combined for an efficient solution. If the pavement response is integrated by the implicit method, then the time step needed for accuracy is usually smaller than the critical time step for the soil. Thus the explicit method can be used for the soil while the implicit method is used for the pavement. The coupling of the implicit and explicit portions of the solution is described in Section 5.4.6.

Chapter 6 compares the results of a falling-weight simulation with data from the Ohio test pavement.

CHAPTER 2

Hexahedral Elements

The finite element program makes available three different hexahedral elements for three-dimensional analysis. These are an eight-node linear element, a twenty-node quadratic element, and an element having a variable number of nodes. Although the eight-node and twenty-node elements have been programmed separately for computational efficiency, they can be considered as special cases of the variable element. Thus only the variable element will be discussed in detail in this chapter. The development of these elements generally follows Bathe [**1**], but the elements described by Weaver [**9**] and Zienkiewicz [**10**] are similar.

2.1. Formulation

The hexahedral element has eight corner nodes and zero to twelve mid-side nodes. The numbering of the nodes is shown in Figure 2.1. In the local ξ–η–ζ coordinate system, the element is a cube situated between -1 and $+1$ in each direction. This is a displacement-based element, which means that interpolation functions are assumed to predict the displacements at any point, given the displacements at the nodes. This is also an isoparametric element, meaning the same functions are used to interpolate the coordinates.

2.1.1. Interpolation. The interpolation functions in each direction can be either linear or quadratic, depending on the presence of mid-side nodes. The interpolation functions are defined in the local ξ–η–ζ coordinates. Because the element is isoparametric, a single set of interpolation functions is used to interpolate any quantity defined at the nodes. For example, the global coordinates (x, y, z) corresponding to any point (ξ, η, ζ) in the element can be found easily by

$$x = \sum_{i=1}^{20} h_i x_i, \quad y = \sum_{i=1}^{20} h_i y_i, \quad z = \sum_{i=1}^{20} h_i z_i, \tag{2.1}$$

where x_i, y_i, z_i are the global coordinates of node i and $h_i\,(\xi, \eta, \zeta)$ is the matching interpolation function. Obviously, undefined nodes need not be included

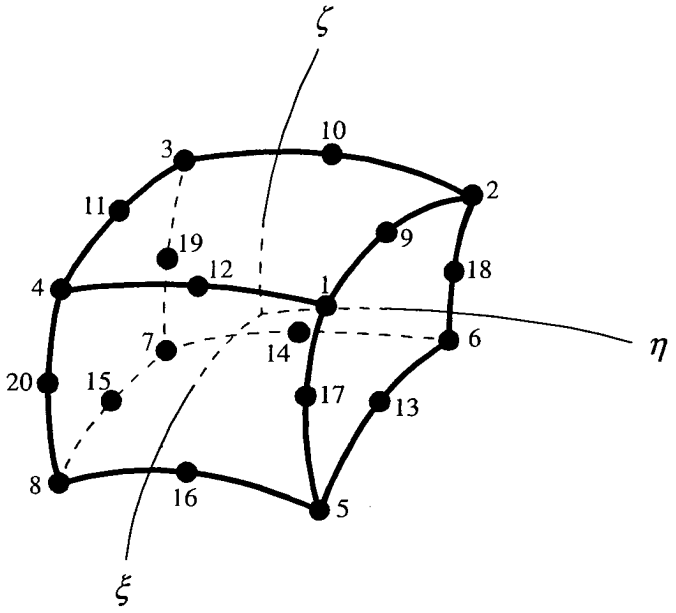

FIGURE 2.1. Twenty-node hexahedral element.

in the summation. Displacements may be interpolated in a similar way:

$$u = \sum_{i=1}^{20} h_i u_i, \quad v = \sum_{i=1}^{20} h_i v_i, \quad w = \sum_{i=1}^{20} h_i w_i. \tag{2.2}$$

Here are the interpolation functions for the corner nodes:

$$\begin{aligned}
h_1 &= \tfrac{1}{8}(1+\xi)(1+\eta)(1+\zeta) - \tfrac{1}{2}(h_9 + h_{12} + h_{17}), \\
h_2 &= \tfrac{1}{8}(1-\xi)(1+\eta)(1+\zeta) - \tfrac{1}{2}(h_9 + h_{10} + h_{18}), \\
h_3 &= \tfrac{1}{8}(1-\xi)(1-\eta)(1+\zeta) - \tfrac{1}{2}(h_{10} + h_{11} + h_{19}), \\
h_4 &= \tfrac{1}{8}(1+\xi)(1-\eta)(1+\zeta) - \tfrac{1}{2}(h_{11} + h_{12} + h_{20}), \\
h_5 &= \tfrac{1}{8}(1+\xi)(1+\eta)(1-\zeta) - \tfrac{1}{2}(h_{13} + h_{16} + h_{17}), \\
h_6 &= \tfrac{1}{8}(1-\xi)(1+\eta)(1-\zeta) - \tfrac{1}{2}(h_{13} + h_{14} + h_{18}), \\
h_7 &= \tfrac{1}{8}(1-\xi)(1-\eta)(1-\zeta) - \tfrac{1}{2}(h_{14} + h_{15} + h_{19}), \\
h_8 &= \tfrac{1}{8}(1+\xi)(1-\eta)(1-\zeta) - \tfrac{1}{2}(h_{15} + h_{16} + h_{20}).
\end{aligned} \tag{2.3}$$

TABLE 2.1. Local coordinates for twenty-node element.

i	ξ_i	η_i	ζ_i	i	ξ_i	η_i	ζ_i	i	ξ_i	η_i	ζ_i
1	1	1	1	9	0	1	1	17	1	1	0
2	−1	1	1	10	−1	0	1	18	−1	1	0
3	−1	−1	1	11	0	−1	1	19	−1	−1	0
4	1	−1	1	12	1	0	1	20	1	−1	0
5	1	1	−1	13	0	1	−1				
6	−1	1	−1	14	−1	0	−1				
7	−1	−1	−1	15	0	−1	−1				
8	1	−1	−1	16	1	0	−1				

The interpolation functions for the mid-side nodes are

$$h_i = \begin{cases} 0 & \text{if node } i \text{ is undefined,} \\ \frac{1}{4}(1-\xi^2)(1+\eta_i\eta)(1+\zeta_i\zeta) & \text{for } i = 9, 11, 13, 15, \\ \frac{1}{4}(1-\eta^2)(1+\xi_i\xi)(1+\zeta_i\zeta) & \text{for } i = 10, 12, 14, 16, \\ \frac{1}{4}(1-\zeta^2)(1+\xi_i\xi)(1+\eta_i\eta) & \text{for } i = 17, 18, 19, 20, \end{cases} \tag{2.4}$$

in which (ξ_i, η_i, ζ_i) is the location of node i in local coordinates. Table 2.1 gives the local coordinates for all twenty nodes.

2.1.2. Strain. The six components of strain at a point are given by derivatives of the displacements u, v, w:

$$\boldsymbol{\varepsilon} = \begin{Bmatrix} \varepsilon_x \\ \varepsilon_y \\ \varepsilon_z \\ \gamma_{xy} \\ \gamma_{yz} \\ \gamma_{zx} \end{Bmatrix} = \begin{bmatrix} \frac{\partial}{\partial x} & 0 & 0 \\ 0 & \frac{\partial}{\partial y} & 0 \\ 0 & 0 & \frac{\partial}{\partial z} \\ \frac{\partial}{\partial y} & \frac{\partial}{\partial x} & 0 \\ 0 & \frac{\partial}{\partial z} & \frac{\partial}{\partial y} \\ \frac{\partial}{\partial z} & 0 & \frac{\partial}{\partial x} \end{bmatrix} \begin{Bmatrix} u \\ v \\ w \end{Bmatrix}. \tag{2.5}$$

Because the displacements at an arbitrary point must be interpolated from the nodal values by equation 2.2, the strains become

$$\boldsymbol{\varepsilon} = \mathbf{B}\mathbf{u} \tag{2.6}$$

in which the matrix $\mathbf{B}$ has the form

$$\mathbf{B} = [\mathbf{B}_1 \quad \mathbf{B}_2 \quad \cdots \quad \mathbf{B}_{20}] \tag{2.7}$$

and $\mathbf{u}$ is the vector of nodal displacements:

$$\mathbf{u} = \{u_1 \quad v_1 \quad w_1 \quad \cdots \quad u_{20} \quad v_{20} \quad w_{20}\}^{\mathrm{T}}. \tag{2.8}$$

When nodes are undefined, their corresponding columns and rows must be deleted from $\mathbf{B}$ and $\mathbf{u}$ respectively.

Each derivative submatrix of $\mathbf{B}$ is formed from the partial derivatives of an interpolation function with respect to global coordinates as follows:

$$\mathbf{B}_i = \begin{bmatrix} \dfrac{\partial h_i}{\partial x} & 0 & 0 \\ 0 & \dfrac{\partial h_i}{\partial y} & 0 \\ 0 & 0 & \dfrac{\partial h_i}{\partial z} \\ \dfrac{\partial h_i}{\partial y} & \dfrac{\partial h_i}{\partial x} & 0 \\ 0 & \dfrac{\partial h_i}{\partial z} & \dfrac{\partial h_i}{\partial y} \\ \dfrac{\partial h_i}{\partial z} & 0 & \dfrac{\partial h_i}{\partial x} \end{bmatrix}. \tag{2.9}$$

However, the interpolation functions are functions of the local coordinates, so the derivatives in equation 2.9 must be written as

$$\begin{aligned} \frac{\partial h_i}{\partial x} &= \frac{\partial h_i}{\partial \xi}\frac{\partial \xi}{\partial x} + \frac{\partial h_i}{\partial \eta}\frac{\partial \eta}{\partial x} + \frac{\partial h_i}{\partial \zeta}\frac{\partial \zeta}{\partial x}, \\ \frac{\partial h_i}{\partial y} &= \frac{\partial h_i}{\partial \xi}\frac{\partial \xi}{\partial y} + \frac{\partial h_i}{\partial \eta}\frac{\partial \eta}{\partial y} + \frac{\partial h_i}{\partial \zeta}\frac{\partial \zeta}{\partial y}, \\ \frac{\partial h_i}{\partial z} &= \frac{\partial h_i}{\partial \xi}\frac{\partial \xi}{\partial z} + \frac{\partial h_i}{\partial \eta}\frac{\partial \eta}{\partial z} + \frac{\partial h_i}{\partial \zeta}\frac{\partial \zeta}{\partial z}. \end{aligned} \tag{2.10}$$

In general, the partial derivatives of the local coordinates with respect to the global coordinates cannot be computed directly. Instead, they must be

evaluated numerically by inverting the Jacobian matrix,

$$\mathbf{J} = \begin{bmatrix} \frac{\partial x}{\partial \xi} & \frac{\partial y}{\partial \xi} & \frac{\partial z}{\partial \xi} \\ \frac{\partial x}{\partial \eta} & \frac{\partial y}{\partial \eta} & \frac{\partial z}{\partial \eta} \\ \frac{\partial x}{\partial \zeta} & \frac{\partial y}{\partial \zeta} & \frac{\partial z}{\partial \zeta} \end{bmatrix}. \tag{2.11}$$

The entries of the Jacobian matrix are obtained from

$$\mathbf{J} = \mathbf{L}\mathbf{X} \tag{2.12}$$

where $\mathbf{L}$ is a matrix of the derivatives of the interpolation functions with respect to the local coordinates,

$$\mathbf{L} = \begin{bmatrix} \frac{\partial h_1}{\partial \xi} & \frac{\partial h_2}{\partial \xi} & \cdots & \frac{\partial h_{20}}{\partial \xi} \\ \frac{\partial h_1}{\partial \eta} & \frac{\partial h_2}{\partial \eta} & \cdots & \frac{\partial h_{20}}{\partial \eta} \\ \frac{\partial h_1}{\partial \zeta} & \frac{\partial h_2}{\partial \zeta} & \cdots & \frac{\partial h_{20}}{\partial \zeta} \end{bmatrix}, \tag{2.13}$$

and $\mathbf{X}$ is a matrix of the nodal coordinates,

$$\mathbf{X} = \begin{bmatrix} x_1 & y_1 & z_1 \\ x_2 & y_2 & z_2 \\ \vdots & \vdots & \vdots \\ x_{20} & y_{20} & z_{20} \end{bmatrix}. \tag{2.14}$$

As with $\mathbf{B}$ and $\mathbf{u}$, appropriate rows and columns must be deleted from $\mathbf{L}$ and $\mathbf{X}$ when some nodes are undefined. The derivatives needed in equations 2.10 are precisely the entries of $\mathbf{J}^{-1}$:

$$\mathbf{J}^{-1} = \begin{bmatrix} \frac{\partial \xi}{\partial x} & \frac{\partial \eta}{\partial x} & \frac{\partial \zeta}{\partial x} \\ \frac{\partial \xi}{\partial y} & \frac{\partial \eta}{\partial y} & \frac{\partial \zeta}{\partial y} \\ \frac{\partial \xi}{\partial z} & \frac{\partial \eta}{\partial z} & \frac{\partial \zeta}{\partial z} \end{bmatrix}. \tag{2.15}$$

2.1.3. Stress. The six components of stress are

$$\boldsymbol{\sigma} = \begin{Bmatrix} \sigma_x \\ \sigma_y \\ \sigma_z \\ \tau_{xy} \\ \tau_{yz} \\ \tau_{zx} \end{Bmatrix} = \mathbf{E}\boldsymbol{\varepsilon} = \mathbf{EBu} \tag{2.16}$$

where $\mathbf{E}$ is the 6×6 material constitutive matrix as discussed in Chapter 4. $\mathbf{E}$ may be independent of stress, strain, and time, as is the case in linear elastic analysis; or it may depend on one or more of those quantities. A dependence of $\mathbf{E}$ on stress or strain is characteristic of a nonlinear analysis. A time-dependent constitutive matrix is used in common viscoelastic formulations, but Chapter 4 describes an alternative formulation in which a constant $\mathbf{E}$ is employed.

2.2. Stiffness

The element stiffness matrix $\mathbf{K}$ relates nodal displacements $\mathbf{u}$ to nodal forces $\mathbf{f}$:

$$\mathbf{Ku} = \mathbf{f}. \tag{2.17}$$

The stiffness matrix is an integral over the volume of the element,

$$\mathbf{K} = \int_V \mathbf{B}^{\mathrm{T}}\mathbf{EB}\, dV = \int\int\int \mathbf{B}^{\mathrm{T}}\mathbf{EB}\, dx\, dy\, dz, \tag{2.18}$$

but because $\mathbf{B}$ is computed in local coordinates, the integration in equation 2.18 must be carried out in local coordinates. The change of variables demands a scaling factor to relate the infinitesimal volumes $d\xi\, d\eta\, d\zeta$ and $dV = dx\, dy\, dz$. The required factor is the Jacobian determinant, $|\mathbf{J}|$:

$$dx\, dy\, dz = |\mathbf{J}|\, d\xi\, d\eta\, d\zeta. \tag{2.19}$$

Then equation 2.18 becomes

$$\mathbf{K} = \int_{-1}^{+1}\int_{-1}^{+1}\int_{-1}^{+1} \mathbf{B}^{\mathrm{T}}\mathbf{EB}\, |\mathbf{J}|\, d\xi\, d\eta\, d\zeta \tag{2.20}$$

in local coordinates. The actual integration is done numerically at Gauss-Legendre sampling points.

2.3. Mass

In dynamic analysis, the inertial forces are given by $\mathbf{M}\ddot{\mathbf{u}}$ where $\mathbf{M}$ is the mass matrix and $\ddot{\mathbf{u}}$ is the nodal acceleration vector. To compute the mass matrix, a matrix $\mathbf{H}$ of the interpolation functions is required such that the three components of displacement at any point in the element may be interpolated from the nodal displacements $\mathbf{u}$ by

$$\begin{Bmatrix} u \\ v \\ w \end{Bmatrix} = \mathbf{H}\mathbf{u}. \tag{2.21}$$

The interpolation matrix $\mathbf{H}$ follows directly from equations 2.2 as

$$\mathbf{H} = \begin{bmatrix} h_1 & 0 & 0 & h_2 & 0 & 0 & \cdots & h_{20} & 0 & 0 \\ 0 & h_1 & 0 & 0 & h_2 & 0 & \cdots & 0 & h_{20} & 0 \\ 0 & 0 & h_1 & 0 & 0 & h_2 & \cdots & 0 & 0 & h_{20} \end{bmatrix}. \tag{2.22}$$

As usual, superfluous columns must be deleted. Then the mass matrix is

$$\mathbf{M} = \int_V \rho\, \mathbf{H}^{\mathrm{T}}\mathbf{H}\, dV \tag{2.23}$$

where ρ is the mass density. The integration is done numerically in local coordinates, as for the stiffness matrix.

The mass matrix in equation 2.23 is called a *consistent* mass matrix because it is constructed according to the interpolation functions. An alternative mass matrix is the *lumped* mass matrix, which has nonzero entries only on the diagonal. The lumped mass matrix is useful for some dynamic solution procedures, and the accuracy difference is negligible for many problems involving eight-node (linear) elements. This is because the consistent mass matrix for the linear element itself has relatively large positive entries on the diagonal and smaller positive entries off the diagonal. On the other hand, the twenty-node element has a more complicated consistent mass matrix with many negative entries, so a lumped mass matrix is a very poor approximation for the higher-order elements.

2.4. Body Forces

If the body force density, $\mathbf{b} = \{b_x \; b_y \; b_z\}$, is constant throughout the element, then the corresponding nodal forces are

$$\mathbf{f}_{\mathrm{b}} = \int_V \mathbf{H}^{\mathrm{T}}\mathbf{b}\, dV. \tag{2.24}$$

Otherwise, if **b** is not constant, it is interpolated at each integration point from the nodal values by

$$\mathbf{b} = \mathbf{H}\,\{b_{1x} \quad b_{1y} \quad b_{1z} \quad \cdots \quad b_{20x} \quad b_{20y} \quad b_{20z}\}^{\mathrm{T}}. \tag{2.25}$$

2.5. Surface Tractions

Surface tractions may be applied to any face of the hexahedral element. Tractions may act either normal to the surface (hydrostatic pressure), tangent to the surface (friction), or in a given direction. In the case of hydrostatic pressure, only the pressure itself is specified. For friction, the stress must be given along with a direction vector; the force is applied in the direction orthogonal to both the surface normal and the direction vector. For the third case, the traction must be given as a three-component vector. In each case, the traction may be constant over the surface, or it may be interpolated from nodal values.

2.5.1. Interpolation on a Surface. Figure 2.2 shows the nodal numbering and the local coordinate system of one face of a hexahedral element. The four corner nodes are mandatory; the mid-side nodes are optional as before. The nodes on the face must be numbered as shown so that the numbers proceed counterclockwise as the face is observed from the exterior of the element. The surface interpolation functions are

$$\begin{aligned}
h_{\mathrm{s}1} &= \tfrac{1}{4}\,(1+\xi)\,(1+\eta) - \tfrac{1}{2}\,(h_{\mathrm{s}5} + h_{\mathrm{s}8})\,,\\
h_{\mathrm{s}2} &= \tfrac{1}{4}\,(1-\xi)\,(1+\eta) - \tfrac{1}{2}\,(h_{\mathrm{s}5} + h_{\mathrm{s}6})\,,\\
h_{\mathrm{s}3} &= \tfrac{1}{4}\,(1-\xi)\,(1-\eta) - \tfrac{1}{2}\,(h_{\mathrm{s}6} + h_{\mathrm{s}7})\,,\\
h_{\mathrm{s}4} &= \tfrac{1}{4}\,(1+\xi)\,(1-\eta) - \tfrac{1}{2}\,(h_{\mathrm{s}7} + h_{\mathrm{s}8})\,,\\
h_{\mathrm{s}5} &= \tfrac{1}{2}\,\left(1-\xi^2\right)\,(1+\eta)\,,\\
h_{\mathrm{s}6} &= \tfrac{1}{2}\,\left(1-\eta^2\right)\,(1-\xi)\,,\\
h_{\mathrm{s}7} &= \tfrac{1}{2}\,\left(1-\xi^2\right)\,(1-\eta)\,,\\
h_{\mathrm{s}8} &= \tfrac{1}{2}\,\left(1-\eta^2\right)\,(1+\xi)\,,
\end{aligned} \tag{2.26}$$

in which the local coordinates (ξ, η) are those given in Table 2.2. Of course, the interpolation function must be zero for a non-existent node.

2.5.2. Hydrostatic Pressure. Hydrostatic pressure is exerted in a direction normal to the surface. For a general curved element, the normal direction varies over each face and should be computed at each integration point on the

TABLE 2.2. Local coordinates for eight-node quadrilateral.

i	ξ_i	η_i
1	1	1
2	−1	1
3	−1	−1
4	1	−1
5	0	1
6	−1	0
7	0	−1
8	1	0

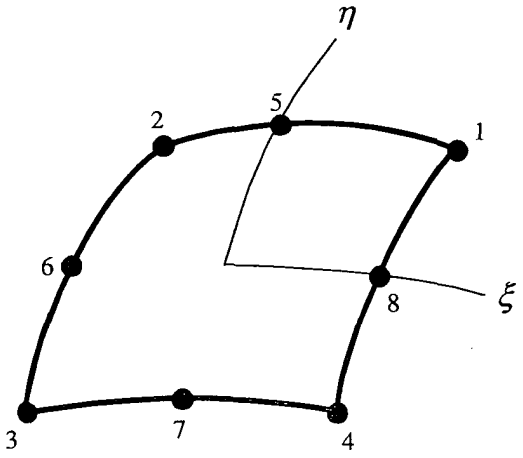

FIGURE 2.2. Local coordinates and node numbers for one face of a twenty-node hexahedral element.

surface. By the chain rule, at any point (ξ, η) on the surface,

$$\begin{Bmatrix} \dfrac{\partial}{\partial \xi} \\ \dfrac{\partial}{\partial \eta} \end{Bmatrix} = \mathbf{J}_\mathrm{s} \begin{Bmatrix} \dfrac{\partial}{\partial x} \\ \dfrac{\partial}{\partial y} \\ \dfrac{\partial}{\partial z} \end{Bmatrix} \tag{2.27}$$

where the Jacobian matrix on the surface is

$$\mathbf{J}_\mathrm{s} = \begin{bmatrix} \dfrac{\partial x}{\partial \xi} & \dfrac{\partial y}{\partial \xi} & \dfrac{\partial z}{\partial \xi} \\ \dfrac{\partial x}{\partial \eta} & \dfrac{\partial y}{\partial \eta} & \dfrac{\partial z}{\partial \eta} \end{bmatrix}. \tag{2.28}$$

Equivalently,

$$\begin{Bmatrix} dx \\ dy \\ dz \end{Bmatrix} = \mathbf{J}_\mathrm{s}^\mathrm{T} \begin{Bmatrix} d\xi \\ d\eta \end{Bmatrix}. \tag{2.29}$$

Thus the two vectors

$$\begin{aligned} \boldsymbol{\xi} &= \begin{Bmatrix} \dfrac{\partial x}{\partial \xi} & \dfrac{\partial y}{\partial \xi} & \dfrac{\partial z}{\partial \xi} \end{Bmatrix}^\mathrm{T}, \\ \boldsymbol{\eta} &= \begin{Bmatrix} \dfrac{\partial x}{\partial \eta} & \dfrac{\partial y}{\partial \eta} & \dfrac{\partial z}{\partial \eta} \end{Bmatrix}^\mathrm{T} \end{aligned} \tag{2.30}$$

define two directions tangent to the surface. It follows that their vector product,

$$\mathbf{n} = \boldsymbol{\xi} \times \boldsymbol{\eta}, \tag{2.31}$$

is normal to the surface.

If $\hat{\mathbf{n}}$ denotes the outward unit normal vector, the force vector resulting from a constant pressure p at any point is $p\,\hat{\mathbf{n}}$. Integration over the surface produces the nodal forces,

$$\mathbf{f}_\mathrm{s} = \int_A p\, \mathbf{H}_\mathrm{s}^\mathrm{T} \hat{\mathbf{n}}\, dA, \tag{2.32}$$

where

$$\mathbf{H}_\mathrm{s} = \begin{bmatrix} h_{\mathrm{s}1} & 0 & 0 & h_{\mathrm{s}2} & 0 & 0 & \cdots & h_{\mathrm{s}8} & 0 & 0 \\ 0 & h_{\mathrm{s}1} & 0 & 0 & h_{\mathrm{s}2} & 0 & \cdots & 0 & h_{\mathrm{s}8} & 0 \\ 0 & 0 & h_{\mathrm{s}1} & 0 & 0 & h_{\mathrm{s}2} & \cdots & 0 & 0 & h_{\mathrm{s}8} \end{bmatrix}. \tag{2.33}$$

Like the volume integrals discussed previously, the integral in equation 2.32 must be computed in local coordinates. The change of variables is accomplished by a scaling factor which relates dA to $d\xi\, d\eta$. This factor is readily determined from the two vectors in equations 2.30; their vector product $\mathbf{n}$ is not only normal to the surface, but its magnitude, $\|\mathbf{n}\| = \sqrt{n_x^2 + n_y^2 + n_z^2}$, is the ratio $dA/\left(d\xi\, d\eta\right)$. Therefore,

$$dA = \|\mathbf{n}\|\, d\xi\, d\eta, \tag{2.34}$$

and the nodal forces are actually integrated as follows:

$$\mathbf{f}_s = \int_{-1}^{+1}\int_{-1}^{+1} p\,\mathbf{H}_s^{\mathrm{T}}\hat{\mathbf{n}}\,\|\mathbf{n}\|\; d\xi\, d\eta = \int_{-1}^{+1}\int_{-1}^{+1} p\,\mathbf{H}_s^{\mathrm{T}}\mathbf{n}\, d\xi\, d\eta. \tag{2.35}$$

If the pressure is not constant, it must be interpolated from the nodal values by

$$p = \mathbf{h}_s \left\{p_1 \quad p_2 \quad \cdots \quad p_8\right\}^{\mathrm{T}} \tag{2.36}$$

where

$$\mathbf{h}_s = \left\{h_{s1} \quad h_{s2} \quad \cdots \quad h_{s8}\right\}. \tag{2.37}$$

2.5.3. Friction. A surface friction is specified by a shearing stress τ and a unit vector $\hat{\mathbf{a}}$. The friction acts in the direction of $\hat{\mathbf{a}} \times \hat{\mathbf{n}}$. The resultant nodal forces are

$$\begin{aligned}\mathbf{f}_s &= \int_A \tau\,\mathbf{H}_s^{\mathrm{T}}\left(\hat{\mathbf{a}} \times \hat{\mathbf{n}}\right)\, dA \\ &= \int_{-1}^{+1}\int_{-1}^{+1} \tau\,\mathbf{H}_s^{\mathrm{T}}\left(\hat{\mathbf{a}} \times \hat{\mathbf{n}}\right)\|\mathbf{n}\|\, d\xi\, d\eta \\ &= \int_{-1}^{+1}\int_{-1}^{+1} \tau\,\mathbf{H}_s^{\mathrm{T}}\left(\hat{\mathbf{a}} \times \mathbf{n}\right) d\xi\, d\eta.\end{aligned} \tag{2.38}$$

Friction may be interpolated by the same method used for hydrostatic pressure (equation 2.37).

2.5.4. Traction in a Specified Direction. A surface traction may be specified as a three-component vector $\mathbf{p} = \left\{p_x \quad p_y \quad p_z\right\}^{\mathrm{T}}$. Each component of $\mathbf{p}$ acts over a *projected* area of the surface. For example, p_x acts on the projection of the face onto the y–z plane. The first component of the unit normal vector, $\hat{n}_x$, is precisely that proportion of the surface area which is projected onto the y–z plane. Similarly, the other components of $\mathbf{p}$ are projected onto

areas given by the other components of $\hat{\mathbf{n}}$. The nodal forces resulting from the surface traction can then be integrated as

$$\mathbf{f}_s = \int_A \mathbf{H}_s^T \mathbf{P} \hat{\mathbf{n}} \, dA, \tag{2.39}$$

where

$$\mathbf{P} = \begin{bmatrix} p_x & 0 & 0 \\ 0 & p_y & 0 \\ 0 & 0 & p_z \end{bmatrix}. \tag{2.40}$$

Integration in local coordinates is accomplished as before:

$$\begin{aligned} \mathbf{f}_s &= \int_{-1}^{+1} \int_{-1}^{+1} \mathbf{H}_s^T \mathbf{P} \hat{\mathbf{n}} \, \|\mathbf{n}\| \, d\xi \, d\eta \\ &= \int_{-1}^{+1} \int_{-1}^{+1} \mathbf{H}_s^T \mathbf{P} \mathbf{n} \, d\xi \, d\eta. \end{aligned} \tag{2.41}$$

If the traction vector is not constant over the entire face, the surface traction must be interpolated from the nodal values by

$$\mathbf{p} = \mathbf{H}_s \{ p_{1x} \quad p_{1y} \quad p_{1z} \quad \cdots \quad p_{8x} \quad p_{8y} \quad p_{8z} \}^T. \tag{2.42}$$

Equation 2.42 performs the same function as equation 2.36 except that equation 2.42 interpolates a vector quantity and equation 2.36 interpolates a scalar quantity.

2.6. Initial Stresses

Initial stresses sometimes arise in special solution procedures. For an initial stress vector $\boldsymbol{\sigma}_0$, the nodal forces are

$$\mathbf{f}_0 = \int_V \mathbf{B}^T \boldsymbol{\sigma}_0 \, dV. \tag{2.43}$$

Then $\boldsymbol{\sigma}_0$ must be subtracted from the stresses computed by equation 2.16 to get effective stresses. Initial stresses are usually known at integration points, but they may be constant throughout the element, or they may be specified at the nodes, with each component interpolated according to equation 2.37.

2.7. Initial Strains

Initial strains can be induced by a temperature change ΔT:

$$\boldsymbol{\varepsilon}_0 = \alpha \, \Delta T \, \{1 \quad 1 \quad 1 \quad 0 \quad 0 \quad 0\}^{\mathrm{T}} \tag{2.44}$$

where α is the coefficient of thermal expansion. Other initial strains can occur as a result of an unusual solution procedure, such as the viscoelastic procedure detailed in Section 4.5. The equivalent nodal forces are

$$\mathbf{f}_0 = \int_V \mathbf{B}^{\mathrm{T}} \mathbf{E} \, \boldsymbol{\varepsilon}_0 \, dV. \tag{2.45}$$

If $\mathbf{E}$ is not constant, $\mathbf{f}_0$ should be updated whenever $\mathbf{E}$ is updated during the solution process. Initial strains must be subtracted from the strains in equation 2.6 before stresses are computed.

For a uniform temperature, the initial strain is constant throughout the entire element. But if the temperature is specified at the nodes, the initial strain must be interpolated from the nodal values. In the case of initial strains arising from a special solution procedure, the values will naturally be available at the integration points.

CHAPTER 3

Axisymmetric Elements

For axisymmetric problems, an isoparametric element of quadrilateral cross section is used [**1, 9, 10**]. It has four corner nodes and four optional mid-side nodes. Specialized, efficiently coded versions are available with four and eight nodes. Axisymmetric problems cannot model a great variety of physical situations, but for those problems that do permit their use, they provide a significantly faster solution without compromising accuracy.

3.1. Formulation

Figure 3.1 shows the cross section of the axisymmetric element. Like the hexahedral element described in Chapter 2, this is an assumed-displacement, isoparametric element. Table 3.1 gives the locations of the nodes in local coordinates. This table is actually a duplicate of Table 2.2.

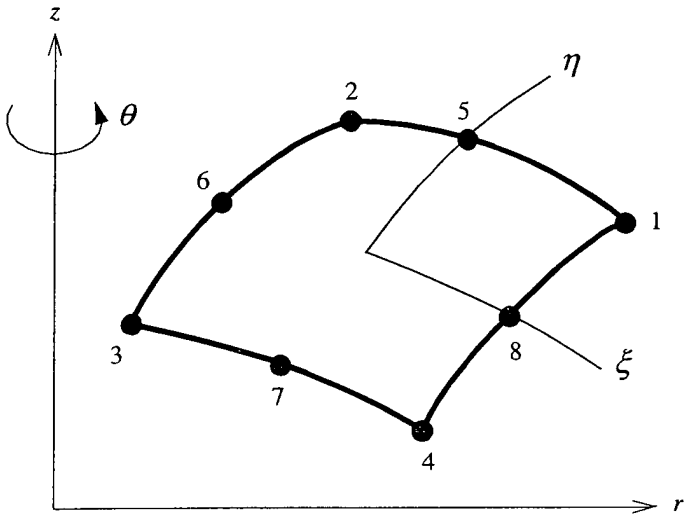

FIGURE 3.1. Eight-node axisymmetric element.

TABLE 3.1. Local coordinates for eight-node axisymmetric element.

i	ξ_i	η_i
1	1	1
2	−1	1
3	−1	−1
4	1	−1
5	0	1
6	−1	0
7	0	−1
8	1	0

3.1.1. Interpolation. The interpolation functions for the axisymmetric element are identical to those introduced in Section 2.5 for a single face of the hexahedral element. They are repeated here for convenience:

$$\begin{aligned}
h_1 &= \tfrac{1}{4}(1+\xi)(1+\eta) - \tfrac{1}{2}(h_5+h_8),\\
h_2 &= \tfrac{1}{4}(1-\xi)(1+\eta) - \tfrac{1}{2}(h_5+h_6),\\
h_3 &= \tfrac{1}{4}(1-\xi)(1-\eta) - \tfrac{1}{2}(h_6+h_7),\\
h_4 &= \tfrac{1}{4}(1+\xi)(1-\eta) - \tfrac{1}{2}(h_7+h_8),\\
h_5 &= \tfrac{1}{2}(1-\xi^2)(1+\eta),\\
h_6 &= \tfrac{1}{2}(1-\eta^2)(1-\xi),\\
h_7 &= \tfrac{1}{2}(1-\xi^2)(1-\eta),\\
h_8 &= \tfrac{1}{2}(1-\eta^2)(1+\xi).
\end{aligned} \tag{3.1}$$

As in Chapter 2, the interpolation functions are zero for unused nodes. Coordinates are interpolated in the usual way,

$$r = \sum_{i=1}^{8} h_i r_i, \quad z = \sum_{i=1}^{8} h_i z_i, \tag{3.2}$$

where, as before, the undefined nodes are excluded from the sums.

The displacements in this formulation include only two components, a radial displacement and an axial displacement; displacement is prohibited in the tangential (θ) direction. The radial component of displacement, along the r direction in Figure 3.1, is denoted by u, and the axial component, in the

direction of z in the figure, is v. This element is isoparametric, so the displacements are interpolated by the same set of functions used in equation 3.2 for the coordinates:

$$u = \sum_{i=1}^{8} h_i u_i, \quad v = \sum_{i=1}^{8} h_i v_i. \tag{3.3}$$

3.1.2. Strain. In the cylindrical r–z–θ coordinate system shown in Figure 3.1, the six strain components are

$$\begin{aligned} \varepsilon_r &= \frac{\partial u}{\partial r}, & \gamma_{rz} &= \frac{\partial u}{\partial z} + \frac{\partial v}{\partial r}, \\ \varepsilon_z &= \frac{\partial v}{\partial z}, & \gamma_{z\theta} &= \frac{1}{r}\frac{\partial v}{\partial \theta} + \frac{\partial w}{\partial z}, \\ \varepsilon_\theta &= \frac{u}{r} + \frac{1}{r}\frac{\partial w}{\partial \theta}, & \gamma_{\theta r} &= \frac{1}{r}\frac{\partial u}{\partial \theta} + \frac{\partial w}{\partial r} - \frac{w}{r}. \end{aligned} \tag{3.4}$$

However, axisymmetry dictates that $w = 0$ and that u and v must be independent of θ. Thus, the strains of interest in this formulation can be written

$$\boldsymbol{\varepsilon} = \begin{Bmatrix} \varepsilon_r \\ \varepsilon_z \\ \varepsilon_\theta \\ \gamma_{rz} \end{Bmatrix} = \begin{bmatrix} \dfrac{\partial}{\partial r} & 0 \\ 0 & \dfrac{\partial}{\partial z} \\ \dfrac{1}{r} & 0 \\ \dfrac{\partial}{\partial z} & \dfrac{\partial}{\partial r} \end{bmatrix} \begin{Bmatrix} u \\ v \end{Bmatrix}. \tag{3.5}$$

When the displacements are interpolated from the nodal values by equation 3.3, the strains become

$$\boldsymbol{\varepsilon} = \mathbf{B}\mathbf{u} \tag{3.6}$$

in which the matrix $\mathbf{B}$ has the form

$$\mathbf{B} = [\mathbf{B}_1 \quad \mathbf{B}_2 \quad \cdots \quad \mathbf{B}_8] \tag{3.7}$$

and $\mathbf{u}$ is the vector of nodal displacements:

$$\mathbf{u} = \{u_1 \quad v_1 \quad \cdots \quad u_8 \quad v_8\}^{\mathrm{T}}. \tag{3.8}$$

The strain should not be computed according to equation 3.6 at the axis of symmetry because the radius, which is zero at the axis, appears in the denominator of the expression for ε_θ. The other strain terms may be evaluated at $r = 0$ if they are desired, but in general strains will be evaluated at the integration points. This precludes the use of Newton–Cotes integration—which places

integration points on the boundary of the integration domain—for elements bordering the axis of symmetry. Gauss–Legendre integration is ordinarily used in the program described in this report, so integration at element boundaries is naturally avoided.

Each derivative submatrix of $\mathbf{B}$ is formed from the partial derivatives of an interpolation function with respect to global coordinates:

$$\mathbf{B}_i = \begin{bmatrix} \dfrac{\partial h_i}{\partial r} & 0 \\ 0 & \dfrac{\partial h_i}{\partial z} \\ \dfrac{h_i}{r} & 0 \\ \dfrac{\partial h_i}{\partial z} & \dfrac{\partial h_i}{\partial r} \end{bmatrix}. \tag{3.9}$$

However, the interpolation functions are defined in terms of the local coordinates, so the derivatives in equation 3.9 must be written as

$$\begin{aligned} \frac{\partial h_i}{\partial r} &= \frac{\partial h_i}{\partial \xi}\frac{\partial \xi}{\partial r} + \frac{\partial h_i}{\partial \eta}\frac{\partial \eta}{\partial r}, \\ \frac{\partial h_i}{\partial z} &= \frac{\partial h_i}{\partial \xi}\frac{\partial \xi}{\partial z} + \frac{\partial h_i}{\partial \eta}\frac{\partial \eta}{\partial z}. \end{aligned} \tag{3.10}$$

In general, the partial derivatives of the local coordinates with respect to the global coordinates cannot be computed directly. Instead, they must be evaluated numerically by inverting the Jacobian matrix of the element cross section,

$$\mathbf{J} = \begin{bmatrix} \dfrac{\partial r}{\partial \xi} & \dfrac{\partial z}{\partial \xi} \\ \dfrac{\partial r}{\partial \eta} & \dfrac{\partial z}{\partial \eta} \end{bmatrix}. \tag{3.11}$$

The entries of the Jacobian matrix are obtained from

$$\mathbf{J} = \mathbf{L}\mathbf{X} \tag{3.12}$$

where $\mathbf{L}$ is a matrix of derivatives of the interpolation functions with respect to the local coordinates,

$$\mathbf{L} = \begin{bmatrix} \dfrac{\partial h_1}{\partial \xi} & \dfrac{\partial h_2}{\partial \xi} & \cdots & \dfrac{\partial h_8}{\partial \xi} \\ \dfrac{\partial h_1}{\partial \eta} & \dfrac{\partial h_2}{\partial \eta} & \cdots & \dfrac{\partial h_8}{\partial \eta} \end{bmatrix}, \tag{3.13}$$

and $\mathbf{X}$ is a matrix of the nodal coordinates,

$$\mathbf{X} = \begin{bmatrix} r_1 & z_1 \\ r_2 & z_2 \\ \vdots & \vdots \\ r_8 & z_8 \end{bmatrix}. \tag{3.14}$$

Now $\mathbf{J}^{-1}$ contains the derivatives needed in equations 3.10:

$$\mathbf{J}^{-1} = \begin{bmatrix} \dfrac{\partial \xi}{\partial r} & \dfrac{\partial \eta}{\partial r} \\ \dfrac{\partial \xi}{\partial z} & \dfrac{\partial \eta}{\partial z} \end{bmatrix}. \tag{3.15}$$

3.1.3. Stress. Four stress components are of interest:

$$\boldsymbol{\sigma} = \begin{Bmatrix} \sigma_r \\ \sigma_z \\ \sigma_\theta \\ \tau_{rz} \end{Bmatrix} = \mathbf{E}\boldsymbol{\varepsilon} = \mathbf{EBu} \tag{3.16}$$

where $\mathbf{E}$ is the 4×4 material constitutive matrix as discussed in Chapter 4.

3.2. Stiffness

The stiffness matrix is integrated over the volume of the element as it is for the hexahedral element (equation 2.18). However, the volume dV here becomes $2\pi r \, |\mathbf{J}| \, d\xi \, d\eta$ in local coordinates. Thus

$$\mathbf{K} = \int_V \mathbf{B}^{\mathrm{T}}\mathbf{EB} \, dV = 2\pi \int_{-1}^{+1} \int_{-1}^{+1} \mathbf{B}^{\mathrm{T}}\mathbf{EB} \, r \, |\mathbf{J}| \, d\xi \, d\eta. \tag{3.17}$$

Of course, r must be interpolated at each integration point by the first of equations 3.2.

3.3. Mass

The integral for the consistent mass matrix looks like the one for the hexahedral element,

$$\mathbf{M} = \int_V \rho \mathbf{H}^{\mathrm{T}} \mathbf{H} \, dV, \tag{3.18}$$

except that $dV = 2\pi r \, |\mathbf{J}| \, d\xi \, d\eta$. Here, $\mathbf{H}$ is the matrix of interpolation functions,

$$\mathbf{H} = \begin{bmatrix} h_1 & 0 & h_2 & 0 & \cdots & h_8 & 0 \\ 0 & h_1 & 0 & h_2 & \cdots & 0 & h_8 \end{bmatrix}, \tag{3.19}$$

which arises naturally from the interpolation of displacements:

$$\begin{Bmatrix} u \\ v \end{Bmatrix} = \mathbf{H}\mathbf{u}. \tag{3.20}$$

A lumped mass matrix may be formed as explained in Chapter 2, but its use should be limited to the four-node element for the reasons discussed in Section 2.3.

3.4. Body Forces

If the body force density, $\mathbf{b} = \{b_r \quad b_z\}$, is defined at the nodes, it is interpolated at each integration point by

$$\mathbf{b} = \mathbf{H} \, \{b_{1r} \quad b_{1z} \quad \cdots \quad b_{8r} \quad b_{8z}\}^{\mathrm{T}}. \tag{3.21}$$

Then the associated nodal forces are

$$\mathbf{f}_{\mathrm{b}} = \int_V \mathbf{H}^{\mathrm{T}} \mathbf{b} \, dV. \tag{3.22}$$

A gravitational force is specified in the component b_z. The radial body force b_r is useful if an axisymmetric body is rotating about its axis of symmetry.

3.5. Surface Tractions

Surface tractions can be applied to any surface of the axisymmetric element, but they must act in the plane of the cross section in Figure 3.1. Thus only r and z components of traction are permitted; the θ component is always zero.

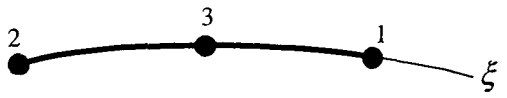

FIGURE 3.2. Node numbers and local coordinate system for one edge of eight-node axisymmetric element.

3.5.1. Interpolation on a Surface. Interpolation on a surface of the axisymmetric element is equivalent to interpolation along an edge of a plane quadrilateral element. In other words, the surface integral is really a line integral scaled by $2\pi r$. Figure 3.2 shows that, along this line, the nodes are renumbered as *1* and *2* at the ends with the optional node *3* in the middle. Node *2* must be located counterclockwise from node *1*—when viewed with the z axis to the left of the cross section—so that the surface normal (equation 3.25) will point outward from the element surface. The local coordinates of the nodes are given in Table 3.2. The surface interpolation functions are

$$\begin{aligned} h_{s1} &= \tfrac{1}{2}\xi\,(\xi+1)\,, \\ h_{s2} &= \tfrac{1}{2}\xi\,(\xi-1)\,, \\ h_{s3} &= 1-\xi^2 \end{aligned} \tag{3.23}$$

if the surface is defined by three nodes, or

$$\begin{aligned} h_{s1} &= \tfrac{1}{2}\,(1+\xi)\,, \\ h_{s2} &= \tfrac{1}{2}\,(1-\xi)\,, \\ h_{s3} &= 0 \end{aligned} \tag{3.24}$$

for two nodes.

TABLE 3.2. Local coordinates for three-node line.

i	ξ_i
1	1
2	−1
3	0

3.5.2. Hydrostatic Pressure. The direction normal (in the r–z plane) to the edge interpolated by functions 3.23 or 3.24 is given by the vector

$$\mathbf{n} = \left\{ -\frac{\partial z}{\partial \xi} \quad \frac{\partial r}{\partial \xi} \right\}^{\mathrm{T}}. \tag{3.25}$$

The nodal forces produced by a hydrostatic pressure p follow as

$$\mathbf{f}_{\mathrm{s}} = \int_A p\, \mathbf{H}_{\mathrm{s}}^{\mathrm{T}} \hat{\mathbf{n}}\, dA, \tag{3.26}$$

where

$$\mathbf{H}_{\mathrm{s}} = \begin{bmatrix} h_{\mathrm{s}1} & 0 & h_{\mathrm{s}2} & 0 & h_{\mathrm{s}3} & 0 \\ 0 & h_{\mathrm{s}1} & 0 & h_{\mathrm{s}2} & 0 & h_{\mathrm{s}3} \end{bmatrix}. \tag{3.27}$$

In the local coordinate system, the differential area becomes $dA = 2\pi r \, \|\mathbf{n}\| \, d\xi$, and hence the nodal forces can be integrated by

$$\mathbf{f}_{\mathrm{s}} = 2\pi \int_{-1}^{+1} p\, \mathbf{H}_{\mathrm{s}}^{\mathrm{T}} \hat{\mathbf{n}}\, r\, \|\mathbf{n}\|\, d\xi = 2\pi \int_{-1}^{+1} p\, \mathbf{H}_{\mathrm{s}}^{\mathrm{T}} \mathbf{n}\, r\, d\xi. \tag{3.28}$$

Of course, r has to be interpolated from the nodes by

$$r = \sum_{i=1}^{3} h_{\mathrm{s}i} r_i, \tag{3.29}$$

and the pressure may be interpolated from nodal values as in Section 2.5.2. It is important to note that a compressive hydrostatic pressure (a positive gage pressure) is indicated by a *negative* value of p.

3.5.3. Friction. The surface friction τ is not permitted to have any θ component; it acts entirely in the ξ direction shown in Figure 3.2. That direction is represented by the tangent vector

$$\mathbf{s} = \left\{ \frac{\partial r}{\partial \xi} \quad \frac{\partial z}{\partial \xi} \right\}^{\mathrm{T}}, \tag{3.30}$$

and the differential area on the surface is $dA = 2\pi r \, \|\mathbf{s}\| \, d\xi$. The consistent nodal forces can then be calculated by

$$\begin{aligned} \mathbf{f}_s &= \int_A \tau \, \mathbf{H}_s^{\mathrm{T}} \hat{\mathbf{s}} \, dA \\ &= 2\pi \int_{-1}^{+1} \tau \, \mathbf{H}_s^{\mathrm{T}} \hat{\mathbf{s}} \, r \, \|\mathbf{s}\| \, d\xi \\ &= 2\pi \int_{-1}^{+1} \tau \, \mathbf{H}_s^{\mathrm{T}} \mathbf{s} \, r \, d\xi. \end{aligned} \tag{3.31}$$

A positive friction tends to rotate the cross section of the element *clockwise* as viewed in Figure 3.1, with the axis of symmetry on the left. Like the hydrostatic pressure, the friction may be interpolated from nodal values, although the utility of this feature is questionable.

3.5.4. Traction in a Specified Direction. When the direction of a surface traction is known, the load $\mathbf{p} = \{p_r \quad p_z\}^{\mathrm{T}}$ can be integrated by

$$\mathbf{f}_s = \int_A \mathbf{H}_s^{\mathrm{T}} \mathbf{P} \hat{\mathbf{s}} \, dA, \tag{3.32}$$

where

$$\mathbf{P} = \begin{bmatrix} p_r & 0 \\ 0 & p_z \end{bmatrix} \tag{3.33}$$

and the load vector $\mathbf{p}$ itself may have to be interpolated from nodal values. The effect of the product $\mathbf{P}\hat{\mathbf{s}}$ is to scale each component of $\mathbf{p}$ by the corresponding component of $\hat{\mathbf{s}}$.

Integration in local coordinates requires a change of variables with $dA = 2\pi r \, \|\mathbf{s}\| \, d\xi$:

$$\begin{aligned} \mathbf{f}_s &= 2\pi \int_{-1}^{+1} \mathbf{H}_s^{\mathrm{T}} \mathbf{P} \hat{\mathbf{s}} \, r \, \|\mathbf{s}\| \, d\xi \\ &= 2\pi \int_{-1}^{+1} \mathbf{H}_s^{\mathrm{T}} \mathbf{P} \mathbf{s} \, r \, d\xi. \end{aligned} \tag{3.34}$$

3.6. Initial Stresses

The equivalent nodal forces produced by initial stresses $\boldsymbol{\sigma}_0$ are

$$\mathbf{f}_0 = \int_V \mathbf{B}^{\mathrm{T}} \boldsymbol{\sigma}_0 \, dV. \tag{3.35}$$

3.7. Initial Strains

Initial strains $\boldsymbol{\varepsilon}_0$ are equivalent to nodal forces

$$\mathbf{f}_0 = \int_V \mathbf{B}^{\mathrm{T}} \mathbf{E}\, \boldsymbol{\varepsilon}_0 \, dV. \tag{3.36}$$

The initial strains induced by a temperature change of ΔT are

$$\boldsymbol{\varepsilon}_0 = \begin{Bmatrix} \varepsilon_r \\ \varepsilon_z \\ \varepsilon_\theta \\ \gamma_{rz} \end{Bmatrix} = \alpha \, \Delta T \begin{Bmatrix} 1 \\ 1 \\ 1 \\ 0 \end{Bmatrix}. \tag{3.37}$$

CHAPTER 4

Material Properties

A linear elastic model and a linear viscoelastic model are provided for analysis of pavement systems. The elastic model allows rapid solution, whereas the viscoelastic model is more realistic.

4.1. Elastic Model

The elastic material is linear and isotropic [8]. Stress and strain are simply related by

$$\boldsymbol{\sigma} = \mathbf{E}\boldsymbol{\varepsilon} \tag{4.1}$$

where $\mathbf{E}$ is constant; that is, $\mathbf{E}$ does not depend on stress, strain, or time. For the three-dimensional hexahedral elements,

$$\mathbf{E} = \frac{E}{(1+\nu)(1-2\nu)} \begin{bmatrix} 1-\nu & \nu & \nu & 0 & 0 & 0 \\ \nu & 1-\nu & \nu & 0 & 0 & 0 \\ \nu & \nu & 1-\nu & 0 & 0 & 0 \\ 0 & 0 & 0 & \frac{1-2\nu}{2} & 0 & 0 \\ 0 & 0 & 0 & 0 & \frac{1-2\nu}{2} & 0 \\ 0 & 0 & 0 & 0 & 0 & \frac{1-2\nu}{2} \end{bmatrix} \tag{4.2}$$

and for the axisymmetric elements,

$$\mathbf{E} = \frac{E}{(1+\nu)(1-2\nu)} \begin{bmatrix} 1-\nu & \nu & \nu & 0 \\ \nu & 1-\nu & \nu & 0 \\ \nu & \nu & 1-\nu & 0 \\ 0 & 0 & 0 & \frac{1-2\nu}{2} \end{bmatrix}. \tag{4.3}$$

In these equations, E and ν are the familiar Young modulus and Poisson ratio.

4.2. Mechanical Viscoelastic Models

Unlike elastic or elastoplastic materials, viscoelastic materials display time-dependent behavior under constant load [**2, 3, 4, 5, 6, 8**]. In general, viscoelastic materials may be linear or nonlinear, but only linear models are considered here. Linearity means the stress–strain relationship is independent of stress and strain (although it is certainly time-dependent), and as a result, superposition is applicable, just as for the linear elastic model. Linear viscoelastic material models are often based on mechanical assemblages of springs and dashpots [**2, 4, 5, 8**]. Two mechanical models are presented in this chapter: the generalized Kelvin solid and the generalized Maxwell solid. Many other models are possible, but any other linear spring–dashpot model can be considered as a special case of one (or both) of these two models. The mechanical models developed in this section describe uniaxial behavior; the results will be generalized to multiaxial behavior in Section 4.4.

4.2.1. Generalized Kelvin Solid. The basic Kelvin element consists of a spring and a dashpot in parallel and is too simple to represent realistic material behavior. It models a limited viscous flow but no elastic response. The generalized Kelvin solid, shown in Figure 4.1, has a spring in series with n Kelvin elements. The spring and the Kelvin elements each experience the same stress, while their strains are additive. With n in the range of 2 to 5, it provides a much more realistic approximation of actual materials than a single Kelvin element. In fact, the generalized Kelvin solid is the most general linear mechanical model for solid-like viscoelastic behavior [**5**].

The single spring R_0 in Figure 4.1 represents the elastic portion of the overall material response. The stress–strain relationship for the spring is simply

$$\varepsilon_0 = \frac{1}{R_0}\sigma. \tag{4.4}$$

Kelvin element i is made up of a spring with elastic constant R_i and a dashpot with viscous parameter η_i. The stress–strain equation for the spring is $\sigma_i^{\mathrm{S}} = R_i\varepsilon_i^{\mathrm{S}}$, and for the dashpot, $\sigma_i^{\mathrm{D}} = \eta_i\dot{\varepsilon}_i^{\mathrm{D}}$. Since the two strains have to be equal ($\varepsilon_i^{\mathrm{S}} = \varepsilon_i^{\mathrm{D}} = \varepsilon_i$) and the sum of the stresses must be σ, the full equation for a single Kelvin element is

$$\sigma = R_i\varepsilon_i + \eta_i\dot{\varepsilon}_i. \tag{4.5}$$

The total strain in the generalized Kelvin solid is

$$\varepsilon = \frac{1}{R_0}\sigma + \sum_{i=1}^{n}\varepsilon_i. \tag{4.6}$$

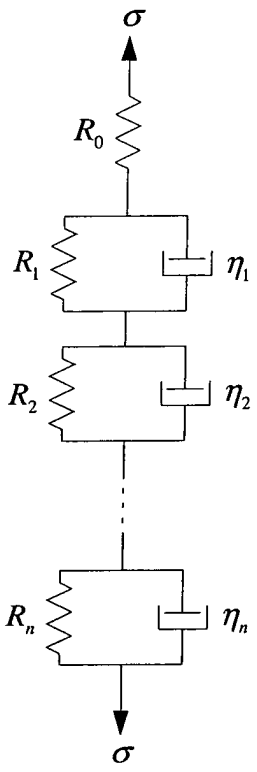

FIGURE 4.1. Generalized Kelvin solid.

Equations 4.5 and 4.6 can be used to find the response of the Kelvin solid to any applied stress or strain.

The creep compliance of this model is easy to derive. In a creep test, a stress is applied suddenly and held constant while the changing strain is measured. Under a constant stress σ_0 applied suddenly at time $t = 0$, the strain in one Kelvin element can be found by integrating equation 4.5 to obtain

$$\varepsilon_i = \frac{\sigma_0}{R_i}\left(1 - e^{-R_i t/\eta_i}\right), \tag{4.7}$$

in which the initial condition $\varepsilon_i(0) = 0$ has been applied. Adding the strains for all the components produces the creep compliance for the generalized Kelvin solid,

$$D = \frac{\varepsilon}{\sigma_0} = D_0 + \sum_{i=1}^{n} D_i\left(1 - e^{-t/\alpha_i}\right), \tag{4.8}$$

where

$$D_0 = \frac{1}{R_0} \tag{4.9}$$

is the elastic compliance and

$$D_i = \frac{1}{R_i}, \tag{4.10}$$

and

$$\alpha_i = \frac{\eta_i}{R_i} \tag{4.11}$$

are called the asymptotic compliance and retardation time for element i. The asymptotic compliance for each element is the value approached as $t \to \infty$, and its retardation time is a measure of how quickly the compliance approaches the limiting value. The compliance of each element i reaches 63 percent of D_i when $t = \alpha_i$.

4.2.2. Generalized Maxwell Solid. Like the simple Kelvin element, the simple Maxwell element is composed of a spring and a dashpot, but the Maxwell element has them arranged in series. Thus the Maxwell element is capable of elastic response, but its viscous flow is fluid-like. Figure 4.2 shows the generalized Maxwell solid, which has n Maxwell elements in parallel with a spring. The single spring acts to limit the viscous flow, making the model solid-like, and the several Maxwell elements provide a range of viscoelastic time constants. The strains in the single spring and in the Maxwell elements must all be equal, whereas the total stress is the sum of the stresses in the individual elements. It will be shown in Appendix A that the generalized Maxwell solid is in fact equivalent to the generalized Kelvin solid.

The stress–strain equation for the single spring in Figure 4.2 is, of course,

$$\sigma_0 = R_0 \varepsilon. \tag{4.12}$$

If the stress in Maxwell element i is σ_i, the strain in spring i is $\varepsilon_i^{\mathrm{S}} = \sigma_i / R_i$, and the strain rate in dashpot i is $\dot{\varepsilon}_i^{\mathrm{D}} = \sigma_i / \eta_i$. Then the total strain is the sum of the spring and dashpot strains, and it must equal ε:

$$\dot{\varepsilon} = \frac{\dot{\sigma}_i}{R_i} + \frac{\sigma_i}{\eta_i}. \tag{4.13}$$

The stress–strain behavior of the entire generalized Maxwell solid under any loading condition is governed by equation 4.13 and the following sum:

$$\sigma = R_0 \varepsilon + \sum_{i=1}^{n} \sigma_i. \tag{4.14}$$

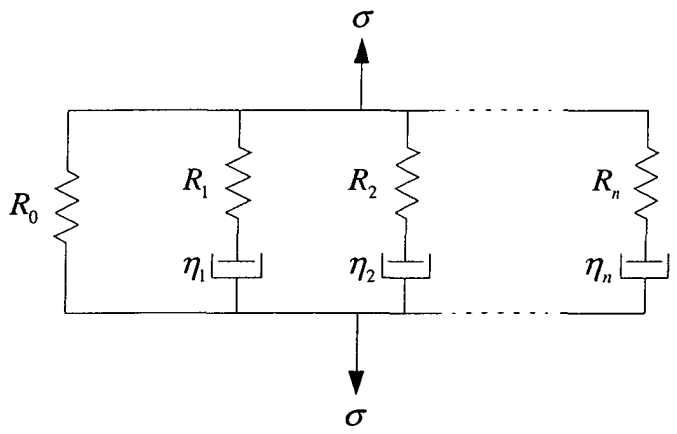

FIGURE 4.2. Generalized Maxwell solid.

In the previous section, the creep compliance was derived for the Kelvin solid, but in this section, the relaxation modulus of the Maxwell solid will be derived. The creep compliance of the Maxwell solid is in fact relatively difficult to derive, as is the relaxation modulus of the Kelvin solid. These will be saved for Appendix A. In a relaxation test, a constant strain ε_0 is applied suddenly at $t = 0$, and the stress is monitored. Obviously, because the strain is constant, $\dot{\varepsilon} = 0$ in equation 4.13. Integration of equation 4.13, using the initial condition $\sigma_i(0) = R_i\varepsilon$, yields

$$\sigma_i = R_i\varepsilon_0 e^{-R_i t/\eta_i}. \tag{4.15}$$

The stresses in all the components can be added to get

$$\frac{\sigma}{\varepsilon_0} = R_0 + \sum_{i=1}^{n} R_i e^{-R_i t/\eta_i}. \tag{4.16}$$

Equation 4.16 can be cast into a more convenient form by letting E_0 be the initial modulus of the overall model,

$$E_0 = R_0 + \sum_{i=1}^{n} R_i, \tag{4.17}$$

and substituting an initial modulus,

$$E_i = R_i, \tag{4.18}$$

and relaxation time,

$$\beta_i = \frac{\eta_i}{R_i} \tag{4.19}$$

for each Maxwell element. The result is the conventional form of the relaxation modulus,

$$E = \frac{\sigma}{\varepsilon_0} = E_0 - \sum_{i=1}^{n} E_i \left(1 - e^{-t/\beta_i}\right). \tag{4.20}$$

4.3. Material Testing

Several laboratory tests can be performed to determine the viscoelastic material properties. The creep and relaxation tests (Section 4.3.1) are the two most elementary tests [**2, 5**], and their results can be put directly in the form of equations 4.8 and 4.20 to get the viscoelastic parameters. The main difficulty with the creep and relaxation tests is that they are relatively long-term tests; they characterize the material response over periods ranging from a few seconds to many years. Cyclic loading tests are more effective when the short-term response is needed [**2, 5**]. Tests involving cyclic stress and strain will be discussed in Section 4.3.2.

4.3.1. Creep and Relaxation Tests. The creep compliance of the generalized Kelvin solid was derived in Section 4.2.1. The result is equation 4.8. A creep test yields strain data at various times after application of the constant stress. The instantaneous strain directly indicates the elastic compliance D_0, but the other parameters must be found by a fitting process. Fitting the experimental data points to equation 4.8 involves, first, selection of the order n of the model; typically, $2 \leq n \leq 5$. Then, in theory, the fitting can be performed with a nonlinear least squares method, but the fit will likely be very ill conditioned. Therefore, it is generally more effective to choose the retardation times α_i and then to find the compliances D_i by a linear least squares method. For example, the retardation times could be selected as powers of two, $\alpha_i = 2^{i+k}$, or powers of ten, $\alpha_i = 10^{i+k}$. The constant k (as well as the number n of Kelvin elements) would depend on the time period of interest.

A similar method can be used to fit relaxation data to equation 4.20. An important fact is that, if the material is truly a linear viscoelastic one, the creep and relaxation tests are redundant. Appendix A will prove this point.

4.3.2. Cyclic Loading Tests. The creep and relaxation tests are not often used to measure the response of materials at times much shorter than one second. This is because the application of the stress or strain cannot be instantaneous. If the load is applied too quickly, undesirable inertial effects

will be induced in the material. On the other hand, the effect of the finite loading rate will become important if the load is applied too slowly relative to the sampling period. A cyclic test circumvents this dilemma by applying a sinusoidal load at frequencies that are well below the resonant frequency of the sample.

A sinusoidal stress will be considered first for the generalized Kelvin solid. It is convenient to write the stress in complex exponential notation as

$$\sigma = \sigma_0 e^{i\omega t}. \tag{4.21}$$

Now the strain in the spring is

$$\varepsilon_0 = \frac{1}{R_0}\sigma_0 e^{i\omega t}, \tag{4.22}$$

and the differential equation 4.5 for each Kelvin element can be solved to get

$$\varepsilon_j = D_j \left(\frac{1 - i\omega\alpha_j}{1 + \omega^2\alpha_j^2} \right) \sigma_0 e^{i\omega t} + Ce^{-t/\alpha_j} \tag{4.23}$$

where C is a constant of integration. Only the steady-state response is relevant, so the last term can be neglected. The total steady-state strain is then

$$\varepsilon = D\sigma_0 e^{i\omega t} \tag{4.24}$$

where D is the complex compliance,

$$D = D_0 + \sum_{j=1}^{n} D_j \left(\frac{1 - i\omega\alpha_j}{1 + \omega^2\alpha_j^2} \right). \tag{4.25}$$

If the complex compliance is written in the form $D = |D| e^{i\delta t}$, then equation 4.24 can be rewritten as

$$\varepsilon = |D| \sigma_0 e^{i(\omega+\delta)t}. \tag{4.26}$$

The magnitude $|D|$ and the phase angle δ are directly measured in the sinusoidal stress test, which should be performed at several frequencies ω. The parameters D_j and α_j can then be found by a nonlinear least-squares fit, or α_j can be fixed as explained in Section 4.3.1 and D_j found by a linear fit.

Similarly, a sinusoidal strain test can be run to obtain the parameters of a generalized Maxwell solid. The strain can be assumed to have the form

$$\varepsilon = \varepsilon_0 e^{i\omega t}. \tag{4.27}$$

The resulting steady-state stresses are

$$\sigma_0 = R_0 \varepsilon_0 e^{i\omega t} \tag{4.28}$$

for the spring and

$$\sigma_j = R_j \beta_j \omega \left(\frac{\beta_j \omega + i}{1 + \omega^2 \beta^2} \right) \varepsilon_0 e^{i\omega t} \tag{4.29}$$

for each Maxwell element. At each frequency ω, a complex modulus is measured:

$$E = |E| \, e^{i\delta t}. \tag{4.30}$$

The parameters $E_j = 1/R_j$ and $\beta_j = \eta_j / R_j$ can be calculated as described for the cyclic stress test.

4.4. Multiaxial Viscoelastic Model

The mechanical viscoelastic models described in Section 4.2 are uniaxial models. For multiaxial stress analysis, more than one model is needed. In the isotropic case, two models are needed: one analogous to the Young modulus and one for the Poisson ratio, for example [**8**]. Alternatively, the bulk and shear moduli can be modeled [**11**]; this is the approach adopted for this project. The advantage of treating bulk and shear phenomena separately is that the volumetric response of many viscoelastic materials is approximately elastic. In other words, often the bulk modulus is assumed constant while only the shear modulus is modeled as viscoelastic. In terms of the bulk modulus K and the shear modulus G, the three-dimensional stress–strain matrix in equation 4.2 is

$$\mathbf{E} = \frac{1}{3} \begin{bmatrix} 3K+4G & 3K-2G & 3K-2G & 0 & 0 & 0 \\ 3K-2G & 3K+4G & 3K-2G & 0 & 0 & 0 \\ 3K-2G & 3K-2G & 3K+4G & 0 & 0 & 0 \\ 0 & 0 & 0 & 3G & 0 & 0 \\ 0 & 0 & 0 & 0 & 3G & 0 \\ 0 & 0 & 0 & 0 & 0 & 3G \end{bmatrix}. \tag{4.31}$$

The corresponding matrix for axisymmetric stress (equation 4.3) is

$$\mathbf{E} = \frac{1}{3} \begin{bmatrix} 3K+4G & 3K-2G & 3K-2G & 0 \\ 3K-2G & 3K+4G & 3K-2G & 0 \\ 3K-2G & 3K-2G & 3K+4G & 0 \\ 0 & 0 & 0 & 3G \end{bmatrix}. \tag{4.32}$$

G and K can be replaced by relaxation moduli of the form

$$G = G_0 - \sum_{i=1}^{n_G} G_i \left(1 - e^{-t/\tau_i^G}\right) \tag{4.33}$$

and

$$K = K_0 - \sum_{i=1}^{n_K} K_i \left(1 - e^{-t/\tau_i^K}\right), \tag{4.34}$$

but the resulting stress–strain relationship will be correct only if the strain is constant. If the stress is constant, the creep compliances are more appropriate:

$$\frac{1}{G} = J = J_0 + \sum_{i=1}^{n_J} J_i \left(1 - e^{-t/\tau_i^J}\right) \tag{4.35}$$

and

$$\frac{1}{K} = B = B_0 + \sum_{i=1}^{n_B} B_i \left(1 - e^{-t/\tau_i^B}\right). \tag{4.36}$$

In a general state of varying stress and strain, the correct moduli will be between these two extremes and will be difficult or impossible to determine exactly. In practice, the stress and strain are computed incrementally, and one or the other is assumed to be constant throughout an increment. Then, for each increment, either the relaxation moduli or the creep compliances can be used, or, as in the next section, the incremental response can be computed from differential equation 4.5 or 4.13.

4.5. Finite Element Implementation

The multiaxial linear viscoelastic model presented in the previous section has been implemented by an elegant method first described by Zienkiewicz et al [**11**]. This method requires the parameters J_0, J_i, τ_i^J, $i = 1, \ldots, n_J$, and B_0, B_i, τ_i^B, $i = 1, \ldots, n_B$, appearing in the creep compliance equations 4.35 and 4.36 for bulk and shear. Strains are separated into elastic and viscoelastic components. The elastic compliances are simply J_0 and B_0, and the elastic moduli are, of course,

$$G_0 = \frac{1}{J_0} \tag{4.37}$$

and

$$K_0 = \frac{1}{B_0}. \tag{4.38}$$

These elastic moduli are used in the **E** matrix in equation 4.31 or 4.32, so the stiffness matrix is independent of time.

The stresses and creep strains are decomposed into average (bulk) and distortional (deviator) components. If a superscript "c" denotes creep strain, the bulk components are

$$\bar{\varepsilon}^{\mathrm{c}} = \frac{1}{3}\left(\varepsilon_x^{\mathrm{c}} + \varepsilon_y^{\mathrm{c}} + \varepsilon_z^{\mathrm{c}}\right) \tag{4.39}$$

and

$$\bar{\sigma} = \frac{1}{3}\left(\sigma_x + \sigma_y + \sigma_z\right), \tag{4.40}$$

and the deviator components are, in vector form,

$$\mathbf{e}^{\mathrm{c}} = \begin{Bmatrix} \varepsilon_x^{\mathrm{c}} - \bar{\varepsilon}^{\mathrm{c}} \\ \varepsilon_y^{\mathrm{c}} - \bar{\varepsilon}^{\mathrm{c}} \\ \varepsilon_z^{\mathrm{c}} - \bar{\varepsilon}^{\mathrm{c}} \\ \frac{1}{2}\gamma_{xy}^{\mathrm{c}} \\ \frac{1}{2}\gamma_{yz}^{\mathrm{c}} \\ \frac{1}{2}\gamma_{zx}^{\mathrm{c}} \end{Bmatrix} \tag{4.41}$$

and

$$\mathbf{s} = \begin{Bmatrix} \sigma_x - \bar{\sigma} \\ \sigma_y - \bar{\sigma} \\ \sigma_z - \bar{\sigma} \\ \tau_{xy} \\ \tau_{yz} \\ \tau_{zx} \end{Bmatrix}. \tag{4.42}$$

The creep strains in the individual elements of the generalized Kelvin models are given by equation 4.5, which is rewritten here in different notation for the bulk and deviatoric components:

$$\dot{\bar{\varepsilon}}_i^{\mathrm{c}} = \frac{B_i}{3\tau_i^B}\bar{\sigma} - \frac{1}{\tau_i^B}\bar{\varepsilon}_i^{\mathrm{c}}, \tag{4.43}$$

$$\dot{\mathbf{e}}_i^{\mathrm{c}} = \frac{J_i}{2\tau_i^J}\mathbf{s} - \frac{1}{\tau_i^J}\mathbf{e}_i^{\mathrm{c}}. \tag{4.44}$$

The creep strains at time $t + \Delta t$ can be approximated from equations 4.43 and 4.44, using the values at t. If the stress is assumed constant throughout

the interval Δt, then equations 4.43 and 4.44 can be integrated to get the approximate creep strains at $t + \Delta t$:

$$(\bar{\varepsilon}_i^c)_{t+\Delta t} = (\bar{\varepsilon}_i^c)_t \, e^{-\Delta t/\tau_i^B} + \tfrac{1}{3} B_i \bar{\sigma}_t \left(1 - e^{-\Delta t/\tau_i^B}\right) \quad i = 1, \ldots, n_B, \tag{4.45}$$

$$(\mathbf{e}_i^c)_{t+\Delta t} = (\mathbf{e}_i^c)_t \, e^{-\Delta t/\tau_i^J} + \tfrac{1}{2} J_i \mathbf{s}_t \left(1 - e^{-\Delta t/\tau_i^J}\right) \quad i = 1, \ldots, n_J. \tag{4.46}$$

The finite element solution advances by time increments of Δt. If at time t, the complete stresses and strains are known (including all the individual components of creep strain), the solution at $t + \Delta t$ proceeds as follows. First, the creep strains at $t + \Delta t$ are found by equations 4.45 and 4.46. All the individual components of those creep strains must be stored. Next, the bulk and deviatoric creep strains are converted to total creep strain, which is treated as an initial strain. This and other initial strains are integrated to get equivalent nodal forces, according to equation 2.45 or 3.36, in which $\mathbf{E}$ represents only the elastic portion of the material response. Then the stiffness matrix is formed at $t + \Delta t$, again using only the elastic matrix $\mathbf{E}$, and all the nodal forces are added together. The solution of the resulting elastic system produces the displacements at $t + \Delta t$, which are used to find the total strain $\boldsymbol{\varepsilon}_{t+\Delta t}$. Finally, the stress $\boldsymbol{\sigma}_{t+\Delta t}$ is given by $\boldsymbol{\sigma}_{t+\Delta t} = \mathbf{E}\left[\boldsymbol{\varepsilon}_{t+\Delta t} - (\boldsymbol{\varepsilon}_0)_{t+\Delta t}\right]$ where $(\boldsymbol{\varepsilon}_0)_{t+\Delta t}$ includes all the initial strains applied at time $t + \Delta t$. The strains calculated from the displacements by equation 2.6 or 3.6 are in fact the *total* strains; they are the sum of the elastic and creep strains.

CHAPTER 5

Finite Element Procedure

In the most general dynamic analysis, element mass and stiffness matrices are assembled into the global matrices $\mathbf{M}$ and $\mathbf{K}$, and element force vectors and concentrated nodal loads are combined into $\mathbf{f}$. The damping matrix $\mathbf{C}$ is constructed from $\mathbf{M}$ and $\mathbf{K}$ as described in Section 5.3. The equation of motion,

$$\mathbf{M}\ddot{\mathbf{u}} + \mathbf{C}\dot{\mathbf{u}} + \mathbf{K}\mathbf{u} = \mathbf{f}, \tag{5.1}$$

is solved at specific increments of time by either an explicit or an implicit method, or by a mixture of the two. The particular methods employed are the central difference method (explicit) and the Newmark trapezoidal method (implicit).

5.1. Central Difference Method

The central difference integration method [**1, 10**] is called an *explicit* method because $\mathbf{u}_{t+\Delta t}$ is written explicitly in terms of the conditions at time t. The central difference method is also called a *conditionally stable* method because its mathematical stability depends upon the size of the time increment used for the step-by-step procedure.

5.1.1. Incremental Procedure. The central difference method gets its name from the second-order difference equation which is assumed for the acceleration at time t,

$$\ddot{\mathbf{u}}_t = \frac{1}{\Delta t^2}\left(\mathbf{u}_{t-\Delta t} - 2\mathbf{u}_t + \mathbf{u}_{t+\Delta t}\right). \tag{5.2}$$

A first-order difference is used for the velocity,

$$\dot{\mathbf{u}}_t = \frac{1}{2\Delta t}\left(-\mathbf{u}_{t-\Delta t} + \mathbf{u}_{t+\Delta t}\right). \tag{5.3}$$

The equilibrium condition at time t follows by substitution of equations 5.2 and 5.3 into equation 5.1:

$$\left(\frac{1}{\Delta t^2}\mathbf{M}+\frac{1}{2\Delta t}\mathbf{C}\right)\mathbf{u}_{t+\Delta t} = \mathbf{f}_t-\left(\mathbf{K}-\frac{2}{\Delta t^2}\mathbf{M}\right)\mathbf{u}_t-\left(\frac{1}{\Delta t^2}\mathbf{M}-\frac{1}{2\Delta t}\mathbf{C}\right)\mathbf{u}_{t-\Delta t}. \quad (5.4)$$

This equation must be solved for $\mathbf{u}_{t+\Delta t}$.

The initial conditions $\mathbf{u}_0$, $\dot{\mathbf{u}}_0$, and $\ddot{\mathbf{u}}_0$ must be specified; they will usually be zero if $\mathbf{f}=\mathbf{0}$ for $t\leq 0$. However, static loads will cause $\mathbf{u}$ to be nonzero, and if loads are to be applied suddenly at $t=0$, the initial acceleration should be computed from equation 5.1. Also required by equation 5.4 is $\mathbf{u}_{-\Delta t}$. Its true value can be determined from the initial loads $\mathbf{f}_{-\infty}$, but equation 5.4 needs a different $\mathbf{u}_{-\Delta t}$ to model accurately the acceleration $\ddot{\mathbf{u}}_0$ produced by the sudden application of loads $\mathbf{f}_0$. It is obtained through the difference equations 5.2 and 5.3, with the result

$$\mathbf{u}_{-\Delta t}=\frac{\Delta t^2}{2}\ddot{\mathbf{u}}_0-\Delta t\dot{\mathbf{u}}_0+\mathbf{u}_0. \quad (5.5)$$

A similar procedure should be used any time loads are applied suddenly instead of gradually.

Equation 5.4 makes it clear that $\mathbf{K}$ never has to be factored. Nevertheless, the matrix $\left(\frac{1}{\Delta t^2}\mathbf{M}+\frac{1}{2\Delta t}\mathbf{C}\right)$ has to be factored, and in general, this matrix is just as difficult to factor as $\mathbf{K}$. For this reason, the central difference method is appealing only when $\mathbf{M}$ is diagonal and $\mathbf{C}$ is diagonal or zero, and thus no matrix factorization is necessary. Otherwise, the implicit integration procedure in Section 5.2 is far more efficient. The central difference method is therefore best used with lumped mass and damping matrices. Chapters 2 and 3 explain that lumped mass should generally not be employed with the quadratic elements, so it follows that the central difference method is most effective with linear elements.

5.1.2. Critical Time Increment. The central difference method is stable only if the time step Δt is less than a critical value [**1, 10**]. Determining that critical value is simple in theory, but computationally expensive in practice. Instead, a lower bound may be found for the critical time step.

If damping is ignored, the equation for free vibration of the finite element mesh is

$$\mathbf{M}\ddot{\mathbf{u}}+\mathbf{K}\mathbf{u}=\mathbf{0}. \quad (5.6)$$

The solution to this equation can be assumed to consist of various modes of vibration, each having a characteristic frequency, phase, and mode shape. Such a solution can be written

$$\mathbf{u} = \boldsymbol{\phi} \sin \omega (t - t_0) \tag{5.7}$$

where $\boldsymbol{\phi}$ is the mode shape vector, ω is the radian frequency of vibration, and t_0 is a constant representing the phase of this mode. Substitution of equation 5.7 into equation 5.6 gives a generalized eigenproblem,

$$\mathbf{K}\boldsymbol{\phi} = \omega^2 \mathbf{M}\boldsymbol{\phi}, \tag{5.8}$$

which has n solutions where n is the number of degrees of freedom in the finite element mesh. Each solution consists of an eigenvector $\boldsymbol{\phi}_i$ and an eigenvalue ω_i^2. The eigenvalues are of particular interest here because the critical time step is

$$\Delta t_{\text{crit}} = \frac{2}{\omega_{\max}} = \frac{T_{\min}}{\pi} \tag{5.9}$$

where $\omega_{\max}$ is the highest natural frequency and $T_{\min} = 2\pi/\omega_{\max}$ is the smallest natural period of vibration.

It is impractical to attempt a direct solution of the eigenproblem of equation 5.8 to obtain $\omega_{\max}$. Instead, an upper bound on $\omega_{\max}$ can be found by a less expensive method [1]. One such method is particularly attractive when a lumped mass matrix is used. In this case, an upper bound on ω^2 is found by rewriting equation 5.8 as

$$\mathbf{M}^{-1}\mathbf{K}\boldsymbol{\phi} = \omega^2 \boldsymbol{\phi} \tag{5.10}$$

and taking norms as follows:

$$\left\|\mathbf{M}^{-1}\right\| \|\mathbf{K}\| \|\boldsymbol{\phi}\| \geq \left\|\mathbf{M}^{-1}\mathbf{K}\boldsymbol{\phi}\right\| = \left|\omega^2\right| \|\boldsymbol{\phi}\| . \tag{5.11}$$

The norms in this equation must be induced vector norms such as the ∞-norm or the 1-norm. Of course, $\mathbf{K}$ is positive definite,

$$\mathbf{x}^{\mathrm{T}}\mathbf{K}\mathbf{x} > 0 \quad \text{for all nonzero } \mathbf{x} \in \Re^n, \tag{5.12}$$

and the eigenvectors can be made $\mathbf{M}$-orthonormal,

$$\boldsymbol{\phi}_i^{\mathrm{T}}\mathbf{M}\boldsymbol{\phi}_j = \delta_{ij}, \tag{5.13}$$

so $\omega^2 > 0$. The resulting upper bound for ω^2 is therefore

$$\omega^2 \leq \left\|\mathbf{M}^{-1}\right\| \|\mathbf{K}\| . \tag{5.14}$$

Now it is clear why this bound is computationally attractive for a lumped mass matrix: the inverse in equation 5.14 becomes trivial.

A second upper bound on ω^2 follows from the fact that the highest natural frequency of the finite element mesh cannot be higher than the highest natural frequency of any single element [**1**]. The matrices $\mathbf{M}$ and $\mathbf{K}$ are manageably small at the element level, and furthermore, many elements typically share common $\mathbf{M}$ and $\mathbf{K}$ matrices, so it is feasible to get an upper bound on ω^2 by equation 5.14—or even to obtain $\omega_{\max}$ directly from equation 5.8—for each element. However, a better upper bound can be obtained by evaluating equation 5.14 for the global mass and stiffness. This operation can be done efficiently at the element level without actually assembling the global matrices.

5.2. Newmark Integration Method

The Newmark method [**1, 10**] is an implicit integration method, which means the displacement vector at time t is computed from the equilibrium equation at time t. Therefore, the disadvantage of this method is that matrix factorization cannot be avoided. On the other hand, Newmark integration has the advantage of being unconditionally stable; that is, the mathematical stability of the procedure does not depend on the time step Δt.

5.2.1. Incremental Procedure. The Newmark method is based on approximations for $\mathbf{u}$ and $\dot{\mathbf{u}}$ of the form

$$\mathbf{u}_{t+\Delta t} = \mathbf{u}_t + \dot{\mathbf{u}}_t \Delta t + \left[\left(\tfrac{1}{2} - \alpha\right) \ddot{\mathbf{u}}_t + \alpha \ddot{\mathbf{u}}_{t+\Delta t}\right] \Delta t^2 \tag{5.15}$$

and

$$\dot{\mathbf{u}}_{t+\Delta t} = \dot{\mathbf{u}}_t + \left[(1 - \delta)\, \ddot{\mathbf{u}}_t + \delta \ddot{\mathbf{u}}_{t+\Delta t}\right] \Delta t \tag{5.16}$$

where α and δ are constants that are selected for accuracy and stability. In the remainder of this chapter, it will be assumed that α and δ are both nonnegative. The trapezoidal rule—with $\alpha = \frac{1}{4}$ and $\delta = \frac{1}{2}$—is commonly used and is unconditionally stable.

Equation 5.15 can be solved for $\ddot{\mathbf{u}}_{t+\Delta t}$ to yield

$$\ddot{\mathbf{u}}_{t+\Delta t} = \frac{1}{\alpha \Delta t^2} \left(\mathbf{u}_{t+\Delta t} - \mathbf{u}_t - \Delta t \dot{\mathbf{u}}_t\right) - \left(\frac{1}{2\alpha} - 1\right) \ddot{\mathbf{u}}_t. \tag{5.17}$$

Substitution of equation 5.17 into equation 5.16 produces

$$\dot{\mathbf{u}}_{t+\Delta t} = \frac{\delta}{\alpha \Delta t} \left(\mathbf{u}_{t+\Delta t} - \mathbf{u}_t\right) + \left(1 - \frac{\delta}{\alpha}\right) \dot{\mathbf{u}}_t + \left(1 - \frac{\delta}{2\alpha}\right) \Delta t \ddot{\mathbf{u}}_t. \tag{5.18}$$

Upon substitution of equations 5.17 and 5.18 into equation 5.1 at time $t+\Delta t$, the equilibrium equation becomes

$$\left(\frac{1}{\alpha\Delta t^2}\mathbf{M}+\frac{\delta}{\alpha\Delta t}\mathbf{C}+\mathbf{K}\right)\mathbf{u}_{t+\Delta t}$$
$$=\mathbf{f}_{t+\Delta t}+\left[\left(\frac{1}{2\alpha}-1\right)\mathbf{M}+\left(\frac{\delta}{2\alpha}-1\right)\Delta t\mathbf{C}\right]\ddot{\mathbf{u}}_t+\left[\frac{1}{\alpha\Delta t}\mathbf{M}+\left(\frac{\delta}{\alpha}-1\right)\mathbf{C}\right]\dot{\mathbf{u}}_t$$
$$+\left(\frac{1}{\alpha\Delta t^2}\mathbf{M}+\frac{\delta}{\alpha\Delta t}\mathbf{C}\right)\mathbf{u}_t. \quad (5.19)$$

To solve equation 5.19 at each increment of time, the matrix

$$\mathbf{A}=\frac{1}{\alpha\Delta t^2}\mathbf{M}+\frac{\delta}{\alpha\Delta t}\mathbf{C}+\mathbf{K} \quad (5.20)$$

must be factored as explained in Section 5.4.5. Then the new velocity and acceleration vectors are obtained from equations 5.18 and 5.17.

Initial conditions for the Newmark method are simpler than for the central difference method in that $\mathbf{u}_{-\Delta t}$ is not needed; only $\mathbf{u}_0$ and $\dot{\mathbf{u}}_0$ need to be specified. The initial acceleration can be specified, or it can be calculated directly from equation 5.1.

5.2.2. Selection of Δt. The stability of the Newmark integration scheme is independent of Δt if α and δ are chosen properly. That leaves accuracy as the criterion governing the selection of Δt. For vibration analysis, Δt should be about one tenth of the shortest period of vibration to be considered [**1**]. However, for pavement, a vibration analysis is not ordinarily useful, but instead a transient analysis must be performed. For a transient analysis, it is necessary to use a time increment that is small enough to provide an accurate representation of the transient response of the system. Experience with nondestructive testing of pavement has shown that a sampling frequency of 1000 Hz is sufficient to obtain a complete trace of pavement response even at 60 mph. Therefore, it is reasonable to believe that $\Delta t = 0.001$ s should suffice for any traffic or falling weight analysis, and longer time increments may be appropriate for simulation of traffic at lower speeds.

5.3. The Damping Matrix

A proper damping matrix cannot be constructed without some knowledge of the dynamic behavior of the overall system. In other words, $\mathbf{C}$ should represent a physically realistic approximation of the velocity-dependent damping

of the entire finite element mesh. A very common form of damping matrix is known as *proportional* damping [1]. If $\mathbf{C}$ is proportional, then

$$\boldsymbol{\phi}_i^{\mathrm{T}} \mathbf{C} \boldsymbol{\phi}_j = 2\omega_i \xi_i \delta_{ij} \tag{5.21}$$

where $\boldsymbol{\phi}_i$ and $\boldsymbol{\phi}_j$ are any two eigenvectors from equation 5.8 and ξ_i is the *damping ratio* for mode i.

5.3.1. Rayleigh Damping. A special case of proportional damping is Rayleigh damping, in which the damping ratio is specified at two different frequencies [1]. The damping matrix is assumed to have the form

$$\mathbf{C} = a\mathbf{M} + b\mathbf{K}, \tag{5.22}$$

so that equation 5.21 becomes

$$\boldsymbol{\phi}_i^{\mathrm{T}} (a\mathbf{M} + b\mathbf{K})\, \boldsymbol{\phi}_i = 2\omega_i \xi_i. \tag{5.23}$$

Equations 5.8 and 5.13 can be used to write equation 5.23 in the form

$$a + b\omega_i^2 = 2\omega_i \xi_i. \tag{5.24}$$

The two constants a and b are evaluated by solving the two simultaneous equations given by equation 5.24 corresponding to the two known damping ratios.

For a mesh composed of different materials, such as a pavement system, each material can have its own set of Rayleigh damping coefficients. The damping ratios should be determined by experiment if possible, because there is no good way to estimate them.

5.3.2. Damping in Explicit Integration. For the central difference method, a diagonal damping matrix should be employed. If $\mathbf{M}$ is diagonal, the Rayleigh damping matrix of equation 5.22 will have the same pattern of nonzero entries as the $\mathbf{K}$ matrix. Thus a further approximation is needed to make $\mathbf{C}$ diagonal. An obvious approach is to use equation 5.22 but with $\mathbf{K}$ replaced by a diagonal matrix $\hat{\mathbf{K}}$. For example, $\hat{\mathbf{K}}$ could contain only the diagonal entries of $\mathbf{K}$, or it could have at each position on the diagonal the sum of the absolute values of the elements in that row of $\mathbf{K}$. In effect, $\hat{\mathbf{K}}$ is a lumped stiffness matrix.

5.3.3. Damping in Implicit Integration. Rayleigh damping has the significant advantage of producing a $\mathbf{C}$ matrix whose bandwidth is no wider than the greater of the bandwidths of $\mathbf{M}$ and $\mathbf{K}$. Thus the use of Rayleigh damping does not increase the work required to factor the matrix $\mathbf{A}$ in equation 5.20. However, precautions must be taken to ensure positive definiteness

of that matrix so that it can be factored. $\mathbf{K}$ is certainly positive definite because of conservation of energy. The consistent mass matrix also is positive definite because of the way it is constructed. It follows that if a and b are both positive, then $\mathbf{C}$ will be positive definite, and so will be $\mathbf{A}$.

The case $a = b = 0$ represents no damping, and $\mathbf{A}$ is clearly positive definite in that case. But if $a < 0$ or $b < 0$, further investigation must be made. It is helpful to rewrite equation 5.20 as

$$\mathbf{A} = \frac{1 + a\delta\Delta t}{\alpha\Delta t^2}\mathbf{M} + \frac{\alpha\Delta t + b\delta}{\alpha\Delta t}\mathbf{K}. \tag{5.25}$$

Now, if the coefficients of $\mathbf{M}$ and $\mathbf{K}$ are both non-negative, $\mathbf{A}$ will be positive definite. In particular, positive definiteness of $\mathbf{A}$ can be guaranteed by ensuring that

$$a \geq -\frac{1}{\delta\Delta t} \tag{5.26}$$

and

$$b \geq -\frac{\alpha\Delta t}{\delta}. \tag{5.27}$$

5.4. The Complete Procedure

The complete solution procedure is outlined below. Most of the individual steps have already been explained in detail. The rest are self-explanatory.

5.4.1. Read the Input Data. The input files are read and checked for consistency. These include a mesh file, a material file, a load file, and a boundary condition file. The mesh file holds data for the nodes and elements, including the coordinates for each node, the node numbers for each element, and the material number for each element. Optional data include integration patterns as well as sets, which are collections of elements or nodes that can be manipulated as a group at a later point in the solution procedure. Examples of sets would be the elements that should be integrated implicitly or explicitly, nodes for which displacements should be output, or elements for which stresses are wanted. The material file specifies the type and properties of each material, the load file list loads of all kinds, and of course, the boundary condition file contains the boundary conditions.

5.4.2. Determine What Type of Analysis Is Required. The input files indicate whether a static or a dynamic analysis is needed. If the problem is dynamic, it must be determined whether to use implicit, explicit, or implicit–explicit integration. Implicit–explicit integration can be used if the time step needed for implicit integration of the stiffest part of the mesh is as short as

that needed for explicit integration of the most flexible part. For a pavement system, this usually implies implicit integration in the pavement and base layers, with explicit integration in the subgrade. If implicit–explicit integration is to be used, the mesh is divided into the parts to be integrated by each method. In addition, the time increment is selected if the analysis is dynamic or if time-dependent (viscoelastic) materials are present.

5.4.3. Compute M, K, and C. The mass, stiffness, and damping matrices are constant throughout the procedure. This is true even for viscoelastic materials because $\mathbf{K}$ represents only the elastic (initial) part of the stress–strain relationship. For a static analysis, only $\mathbf{K}$ is computed. The equations for the explicitly integrated degrees of freedom do not need to be included in $\mathbf{K}$. In the case of implicit–explicit integration, $\mathbf{M}$ and $\mathbf{C}$ are each split into two parts; the parts for the explicitly integrated degrees of freedom are diagonal.

5.4.4. Compute the Initial Conditions. The initial force vector $\mathbf{f}_{-\infty}$ is initialized. These are the forces applied for a relatively long time before $t = 0$, such as body forces, long-term thermal strains, and other static loads. Two initial displacement vectors $\mathbf{u}_{-\infty}$ and $\mathbf{u}_0$ are set by a static analysis using the forces $\mathbf{f}_{-\infty}$. The vector $\mathbf{u}_{-\infty}$ is the instantaneous displacement due to initial forces and is computed with the usual $\mathbf{K}$ matrix. The corresponding stresses and strains are $\boldsymbol{\sigma}_{-\infty}$ and $\boldsymbol{\varepsilon}_{-\infty}$. Displacement $\mathbf{u}_0$ at $t = 0$ is computed with a different stiffness matrix, $\mathbf{K}_\infty$, which is obtained by substituting $\mathbf{E}_\infty$ for $\mathbf{E}$ in the stiffness calculation. $\mathbf{E}_\infty$ is formed by letting t approach ∞ in equations 4.35 and 4.36. The resulting displacements, strains, and stresses are $\mathbf{u}_0$, $\boldsymbol{\varepsilon}_0$, and $\boldsymbol{\sigma}_0 = \mathbf{E}_\infty \boldsymbol{\varepsilon}_0$. Initial creep strains are $\boldsymbol{\varepsilon}_0^c = \boldsymbol{\varepsilon}_0 - \mathbf{E}_0^{-1}\boldsymbol{\sigma}_0$.

The initial velocity $\dot{\mathbf{u}}_0$ is set to zero, and the initial acceleration $\ddot{\mathbf{u}}_0$ is calculated by equation 5.1 using $\mathbf{f}_0$. If $\mathbf{M}$ is not a lumped mass matrix, it has to be factored to find $\ddot{\mathbf{u}}_0$. In general this operation is as expensive as factoring $\mathbf{K}$ (or $\mathbf{A}$ in equation 5.20). If some degrees of freedom are to be integrated explicitly, the initial condition $\mathbf{u}_{-\Delta t}$ is evaluated by equation 5.5.

5.4.5. Perform the Matrix Factorization. In a static analysis, $\mathbf{K}$ is factored. In dynamic problems, the matrix $\mathbf{A}$ in equation 5.20 is formed for the implicitly integrated degrees of freedom and then factored. In either case, an $\mathbf{LDL}^T$ factorization is used. No factorization is necessary for the explicit integration.

5.4.6. Solve for Displacements. A static, linear elastic problem simply requires a single solution of $\mathbf{Ku} = \mathbf{f}$. On the other hand, a problem involving viscoelastic materials, time-dependent loads, or dynamic effects, demands an incremental solution at discrete multiples of Δt. At each time step t, the

force vector $\mathbf{f}_t$ is assembled for a quasistatic problem or for the implicit part of a dynamic problem. Then the equilibrium condition is imposed and the displacements are found. In the quasistatic case, the equilibrium condition is just $\mathbf{K}\mathbf{u}_t = \mathbf{f}_t$.

Integration of the equation of motion for a dynamic problem is more involved. The steps are detailed here for the most general implicit–explicit integration procedure; the procedures for implicit and explicit integration alone are obvious special cases of this more general procedure. First the explicit integration step (equation 5.4) is carried out to get the explicitly integrated part of $\mathbf{u}_{t+\Delta t}$. If any load is to be applied suddenly at t, the procedure described in Section 5.1.1 is used to find the additional acceleration to add to $\ddot{\mathbf{u}}_t$ and the resulting displacement to add to $\mathbf{u}_{t-\Delta t}$. The right-hand side of equation 5.4 is actually formed at the element level, without ever assembling the relevant part of the global stiffness matrix. In general, the vectors $\mathbf{u}_t$ and $\mathbf{u}_{t-\Delta t}$ used for the explicit step include displacement components from some of the implicitly integrated degrees of freedom. In other words, there is some coupling between the explicit and implicit integration operations. To finish the explicit integration step, the relevant parts of the acceleration and velocity vectors are calculated by equations 5.2 and 5.3. After the explicit step has been completed, the implicit integration step is carried out (equation 5.19). Again, the coupling between the explicit and implicit degrees of freedom must be considered. For the explicitly integrated degrees of freedom in equation 5.19, the values that were just computed are used. Finally, the acceleration and velocity are updated by equations 5.17 and 5.18.

The incremental procedure, whether static or dynamic, is continued until the maximum time of interest has been reached. At each increment of time, the load vector $\mathbf{f}_t$ may have to be updated to reflect varying loads, moving loads, or viscoelastic creep strains.

5.4.7. Compute Strains and Stresses. After each increment of time, total strains are computed at the integration points according to equation 2.6 or 3.6. Viscoelastic strains (which are computed as in Section 4.5) and other initial strains are subtracted from the total strains to obtain effective strains. Total stresses follow by substituting effective strains into equation 2.16 or 3.16. Any initial stresses must be subtracted to get effective stresses.

5.4.8. Print the Results. The nodal displacements as well as the stresses and strains at each integration point are printed after each time step.

CHAPTER 6

Sample Problem

This chapter presents the results of a falling-weight simulation which was solved with both elastic and viscoelastic material models. Finite element results are compared with experimental data from the Ohio test pavement section 390106. The falling-weight test occurred on 1999 October 12. The nominal load was 53 kN. A pressure cell and a geophone measured the actual load and the deflection of the pavement. Section 390106 is 180 mm of asphalt on 200 mm of asphalt-treated base and 100 mm of dense graded aggregate.

A mesh of four-node axisymmetric elements extended to 3 m in the radial direction and 3 m deep. The load was applied uniformly over a circle of radius 152 mm as in the falling-weight apparatus. Table 6.1 gives the assumed elastic properties of each layer. The viscoelastic constants of the asphalt layers are listed in Table 6.2.

Figure 6.1 compares the result of the elastic solution with the geophone data. Figure 6.2 shows that the viscoelastic solution is much closer to the experimental measurements.

TABLE 6.1. Elastic material properties of each layer of the sample problem.

Layer	Thickness mm	E MPa	ν
AC	180	3100	0.35
ATB	200	3100	0.35
DGAB	100	170	0.35
Subgrade		70	0.40

TABLE 6.2. Viscoelastic parameters for the sample problem.

i	J_i/J_∞	τ_i (s)
0	0.066	0.0
1	0.026	0.001
2	0.053	0.002
3	0.276	0.003
4	0.434	0.004
5	0.145	0.005

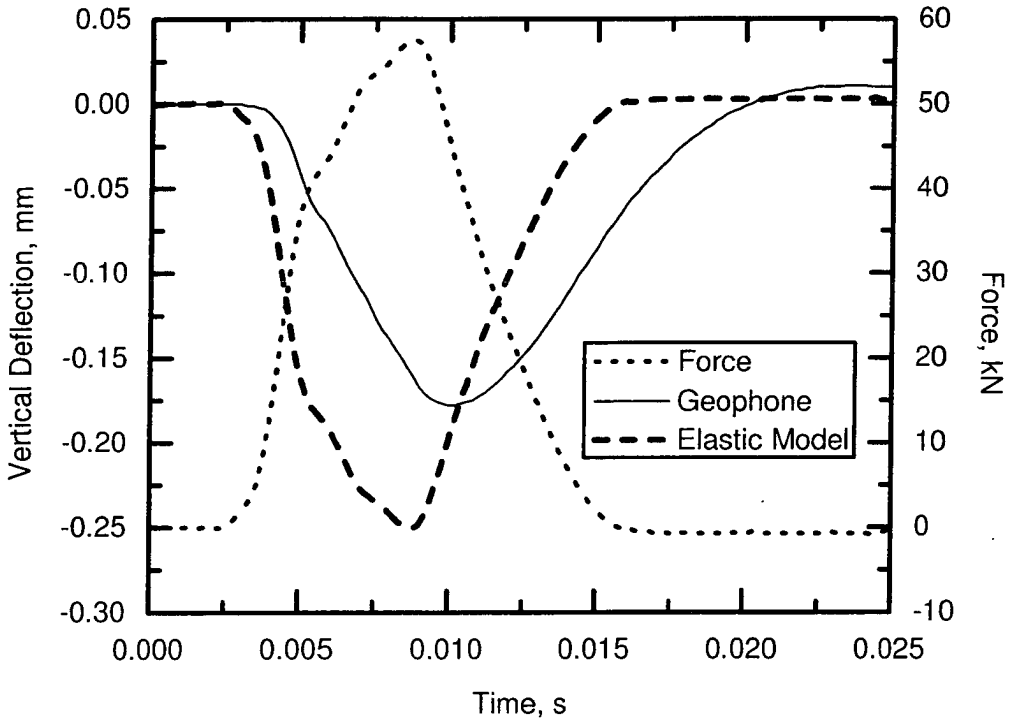

FIGURE 6.1. Elastic solution compared with geophone data.

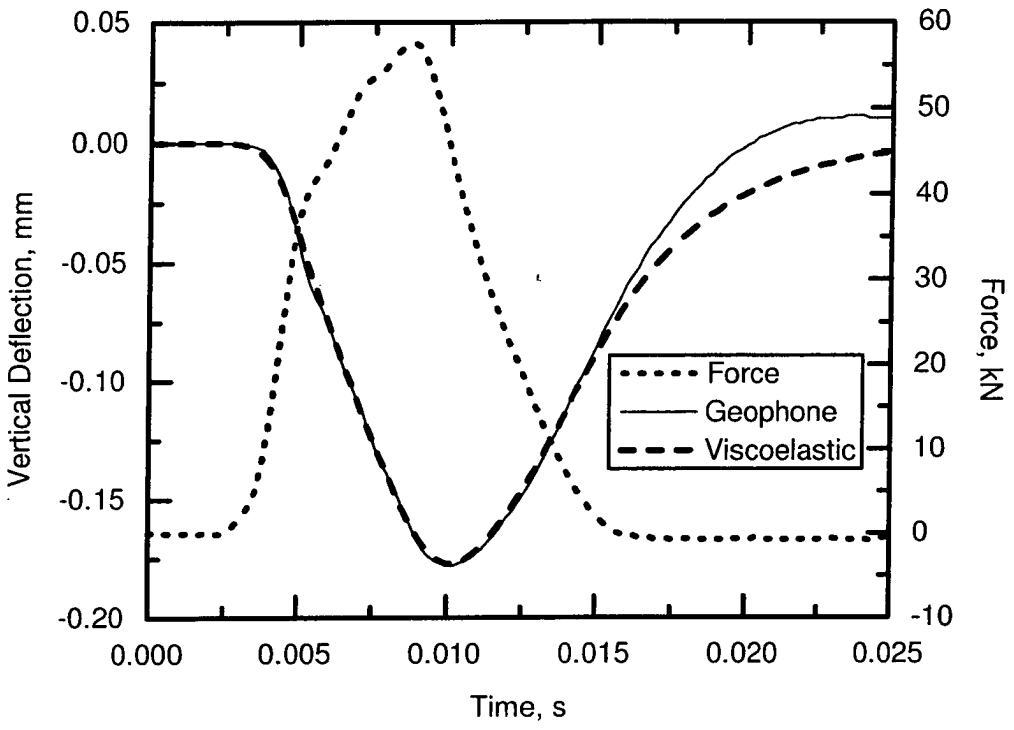

FIGURE 6.2. Viscoelastic solution compared with geophone data.

CHAPTER 7

Conclusions

The sample problem presented in Chapter 6 clearly demonstrates that a linear viscoelastic model can be significantly superior to a linear elastic model, but further research is needed to study the importance of viscoelastic phenomena in real pavements. Two obstacles make that difficult.

First, the viscoelastic material properties need to be determined by laboratory testing. The properties used in Chapter 6 are only approximate values for a typical pavement. Actual viscoelastic constants for several pavement sections should eventually be used to verify the ability of the program to provide accurate predictions of pavement response under a wide range of loading and environmenal conditions. Laboratory tests of asphalt must be conducted at several different temperatures to obtain a realistic viscoelastic model. (The program can be used to solve problems at different temperatures by providing the viscoelastic parameters discussed in Chapter 4 at the desired temperature.) Furthermore, the true behavior of the soil should be considered carefully. Soil can easily be modeled as viscoelastic, but the use of more realistic nonlinear models is not currently feasible because of extremely long solution times.

Indeed, long solution times are the second obstacle impeding further viscoelastic pavement modeling. Realistic problems can require several days or weeks to complete on ordinary desktop computers. An ideal environment for serious pavement modeling would employ specialized compution servers to solve useful problems in a few hours.

APPENDIX A

Equivalence of Kelvin and Maxwell Solids

In Chapter 4, the creep compliance of the generalized Kelvin solid and the relaxation modulus of the generalized Maxwell solid were derived. In this appendix, the Maxwell solid is shown to have a creep compliance of the same form as the Kelvin solid.

The generalized Maxwell solid is shown in Figure A.1. All the Maxwell elements experience the same strain, and the strain rate is, from Equation 4.13,

$$\dot{\varepsilon} = \frac{\dot{\sigma}_i}{R_i} + \frac{\sigma_i}{\eta_i}, \quad i = 1, \ldots, n. \tag{A.1}$$

This equation can be rewritten as

$$\dot{\sigma}_i + \frac{1}{\beta_i}\sigma_i = E_i\dot{\varepsilon}, \quad i = 1, \ldots, n \tag{A.2}$$

by using equations 4.18 and 4.19.

The stress in the lone spring is simply $R_0\varepsilon$, and it is important to observe that this will not be written as σ_0. In Section 4.2.1, σ_0 was used to represent the stress in the lone spring and also the constant stress of the creep test.

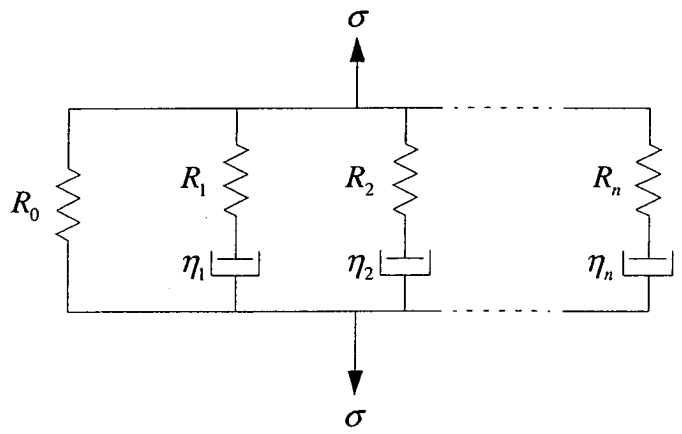

FIGURE A.1. Generalized Maxwell solid.

Likewise, in Section 4.2.2, ε_0 was the strain in the separate spring as well as the constant strain of the relaxation test. In this appendix, however, σ_0 represents only the constant creep stress, and the stress in the single spring is $R_0\varepsilon$.

Now the creep compliance of the Maxwell solid is assumed to have the form of equation 4.8:

$$D = \frac{\varepsilon}{\sigma_0} = D_0 + \sum_{i=1}^{n} D_i \left(1 - e^{-t/\alpha_i}\right). \tag{A.3}$$

Then the strain rate is

$$\dot{\varepsilon} = \sigma_0 \sum_{i=1}^{n} \frac{D_i}{\alpha_i} e^{-t/\alpha_i}, \tag{A.4}$$

and equation A.2 becomes

$$\dot{\sigma}_i + \frac{1}{\beta_i}\sigma_i = E_i\sigma_0 \sum_{j=1}^{n} \frac{D_j}{\alpha_j} e^{-t/\alpha_j}. \tag{A.5}$$

Integration of this equation with the initial condition $\sigma_i(0) = E_i\varepsilon(0)$ produces the following expression for stress in Maxwell element i:

$$\sigma_i = E_i\beta_i\sigma_0 \sum_{j=1}^{n} \frac{D_j}{\alpha_j - \beta_i} e^{-t/\alpha_j} + E_i \left[\varepsilon(0) - \beta_i\sigma_0 \sum_{j=1}^{n} \frac{D_j}{\alpha_j - \beta_i}\right] e^{-t/\beta_i}. \tag{A.6}$$

Differentiation with respect to time yields

$$\dot{\sigma}_i = E_i\sigma_0 \sum_{j=1}^{n} \frac{D_j}{\alpha_j - \beta_i} e^{-t/\beta_i} - \frac{E_i}{\beta_i}\varepsilon(0)e^{-t/\beta_i} - E_i\beta_i\sigma_0 \sum_{j=1}^{n} \frac{D_j}{\alpha_j^2 - \alpha_j\beta_i} e^{-t/\alpha_j}. \tag{A.7}$$

The total stress is the sum of the stresses in the individual elements, and the derivative of the total stress must be zero:

$$\begin{aligned} 0 = \dot{\sigma} &= R_0\dot{\varepsilon} + \sum_{i=1}^{n} \dot{\sigma}_i \\ &= R_0\sigma_0 \sum_{j=1}^{n} \frac{D_j}{\alpha_j} e^{-t\alpha_j} \\ &\quad + \sum_{i=1}^{n} \left[E_i\sigma_0 \sum_{j=1}^{n} \frac{D_j}{\alpha_j - \beta_i} e^{-t/\beta_i} - \frac{E_i}{\beta_i}\varepsilon(0)e^{-t/\beta_i} \right. \\ &\quad \left. - E_i\beta_i\sigma_0 \sum_{j=1}^{n} \frac{D_j}{\alpha_j^2 - \alpha_j\beta_i} e^{-t/\alpha_j} \right]. \end{aligned} \tag{A.8}$$

For this equation to hold at all times t, the coefficients of e^{-t/α_j} and e^{-t/β_i} must be zero. For e^{-t/α_j},

$$\frac{R_0\sigma_0 D_j}{\alpha_j} - \sigma_0 \sum_{i=1}^{n} E_i\beta_i \frac{D_j}{\alpha_j^2 - \alpha_j\beta_i} e^{-t/\alpha_j} = 0, \quad j = 1, \ldots, n \tag{A.9}$$

so that

$$\sum_{i=1}^{n} \frac{E_i\beta_i}{\alpha_j - \beta_i} = R_0, \quad j = 1, \ldots, n. \tag{A.10}$$

Ths initial modulus of the generalized Maxwell solid is given in equation 4.17 as

$$E_0 = R_0 + \sum_{i=1}^{n} R_i. \tag{A.11}$$

Substitution into equation A.10 results in

$$\alpha_j \sum_{i=1}^{n} \frac{E_i}{\alpha_j - \beta_i} = E_0, \quad j = 1, \ldots, n. \tag{A.12}$$

For the e^{-t/β_i} terms,

$$E_i\sigma_0 \sum_{j=1}^{n} \frac{D_j}{\alpha - j - \beta_i} - \frac{E_i}{\beta_i}\varepsilon(0) = 0, \quad i = 1, \ldots, n, \tag{A.13}$$

which leads to

$$\beta_i \sum_{j=1}^{n} \frac{D_j}{\alpha_j - \beta_i} = D_0, \quad i = 1, \ldots, n, \tag{A.14}$$

where

$$D_0 = \frac{\varepsilon(0)}{\sigma_0} = \frac{1}{E_0}. \tag{A.15}$$

Therefore, the equations in this appendix not only demonstrate the equivalence of the generalized Kelvin and Maxwell solids, but they provide a method for converting between the creep compliance and the relaxation modulus. In particular, to convert from creep compliance (equation 4.8) to relaxation modulus (equation 4.20), the time constants β_i are the n roots of equation A.14, the initial modulus is $E_0 = 1/D_0$, and the moduli E_i are given by the n simultaneous equations A.12. To go from relaxation modulus to creep compliance, the time constants α_j are the n roots of equation A.12, the initial compliance is $D_0 = 1/E_0$, and the component compliances D_j are given by n simultaneous equations A.14.

The one difficulty remaining is the solution of equation A.12 for α_j or of equation A.14 for β_i. A general-purpose root-finding method such as Newton–Raphson can be used, but such methods are not foolproof [7]. Specifically, it is usually very helpful to bracket a root before using a general-purpose method, but that cannot be done without some kind of search algorithm. Furthermore, there is no way to guarantee that a bracketed root is not in fact three roots or any odd number of roots. On the other hand, foolproof methods do exist for finding all the roots of a polynomial; Laguerre's method is a good example [7]. Therefore it is helpful to cast equations A.12 and A.14 into polynomial form, and this can in fact be done.

To solve equation A.12 for the n time constants α_j, it is necessary to find the n roots of

$$\alpha \sum_{i=1}^{n} \frac{E_i}{\alpha - \beta_i} - E_0 = 0. \tag{A.16}$$

This equation can be made a polynomial by multiplying it by the product of all n denominators, $\prod_{j=1}^{n}(\alpha - \beta_j)$. The resulting polynomial is

$$\alpha \sum_{i=1}^{n} \left[E_i \prod_{\substack{j=1 \\ j \neq i}}^{n} (\alpha - \beta_j) \right] - E_0 \prod_{j=1}^{n} (\alpha - \beta_j), \tag{A.17}$$

which is obviously of degree n. Laguerre's method, along with polynomial deflation, is guaranteed to find all n roots if exact arithmetic is used. A similar polynomial can be derived from equation A.14.

Unfortunately, the polynomial form of equation A.12 or A.14 will always be ill-conditioned when the time constants are widely distributed. The same is true of the n simultaneous equations. If a "foolproof" method like Laguerre fails to find n roots, then it is necessary either to reduce the number of time constants or to increase the precision of the computations.

References

[1] Klaus-Jürgen Bathe, *Finite Element Procedures in Engineering Analysis*, Prentice–Hall, Englewood Cliffs, New Jersey, 1982.

[2] D. R. Bland, *The Theory of Linear Viscoelasticity*, Pergamon Press, New York, 1960.

[3] R. M. Christensen, *Theory of Viscoelasticity: An Introduction*, Academic Press, New York, 1971.

[4] T. J. Chung, *Continuum Mechanics*, Prentice–Hall, Englewood Cliffs, New Jersey, 1988.

[5] William N. Findley, James S. Lai, and Kasif Onaran, *Creep and Relaxation of Nonlinear Viscoelastic Materials*, Dover Publications, New York, 1989.

[6] Allen C. Pipkin, *Lectures on Viscoelasticity Theory*, Springer–Verlag, New York, 1972.

[7] William H. Press, Saul A. Teukolsky, William T. Vetterling, and Brian P. Flannery, *Numerical Recipes in Fortran*, second edition, Cambridge University Press, Cambridge, 1992.

[8] Irving H. Shames and Francis A. Cozzarelli, *Elastic and Inelastic Stress Analysis*, Taylor and Francis, Washington, D. C., 1997.

[9] William Weaver Jr. and Paul R. Johnston, *Finite Elements for Structural Analysis*, Prentice–Hall, Englewood Cliffs, New Jersey, 1984.

[10] O. C. Zienkiewicz, *The Finite Element Method*, third edition, McGraw–Hill, London, 1977.

[11] O. C. Zienkiewicz, M. Watson, and I. P. King, "A Numerical Method of Visco-Elastic Stress Analysis," *International Journal of Mechanical Sciences*, Vol. 10, pages 807–827, 1968.

ORITE • 114 Stocker Center • Athens, Ohio 45701-2979 • 740-593-2476
Fax: 740-593-0625 •orite@bobcat.ent.ohiou.edu •http://webce.ent.ohiou.edu//orite/